行政院國家科學委員會專題研究計畫成果報告

廣義的機會式通訊：無線行動網路中之競爭、合作與感知-

子計畫一:感知無線行動網路之頻譜偵測與管理

Generalized Opportunistic Communications: Competition, Cooperation and Cognition in Wireless Mobile Networks: Spectrum sensing and management in cognitive wireless mobile networks

計畫編號：**NSC 96-2221-E-009-076-MY3**

執行期間： **98/08/01~99/07/31**

主持人：蘇育德教授 國立交通大學電信工程學系

計畫參與人員：劉人仰、

中文摘要：

在本計畫報告中，我們將總結這三年來的研究所果。本計畫名稱爲：動態頻譜偵測與無線電資源管理之感知傳輸設計。在第一年的研究中，我們著重在探討頻譜估測錯誤的影響。再接下來的兩年，我們則針對不同通訊系統考慮資源分配的問題。由於第一年和第二年的研究成果已經在之前的期中報告中報告過，爲了避免過渡冗長，我們將只摘錄第一年和第二年的重要成果。在第三年的研究中我們探討如何有效的配置空間、頻率以及使用者這三個維度的資源使得用戶的傳輸功率與平均的位元錯誤率降到最低。我們提出兩種以奇異值分解(singular value decomposition)爲基礎的預先編碼技術（分爲正交和非正交兩種）。在第一種方法中，我們將利用奇異值向量的線性組合來合成預先編碼向量以建立多個正交通道（正交預先編碼技術）。之後，我們提出的非正交預先編碼技術則把通道矩陣的秩(rank)限制移除，以增加頻譜使用效率。雖然這將會讓空間通道間產生干擾，而讓資源配置的問題因需滿足某些訊號干擾比之要求而更加複雜，但透過適當的設計，仍可將用戶間的干擾控制在一定的範圍下。針對這兩種預先編碼技術我們分別提出不同的動態資源分配演算法讓用戶的總傳輸功率降到最低。

除此之外，我們還針對實用的碼書(codebook)預先編碼技術之資源配置進行探討，我們提出了動態的子載波分配及傳送功率調整等兩種基本方式及其組合來讓用戶的平均位元錯誤率降到最低。

關鍵詞：頻譜偵測，資源管理，多輸入多輸出-正交分頻多重存取系統。

Abstract

This report documents our effort and findings for the NSC project entitled "Spectrum sensing and management in cognitive wireless mobile networks" during the period 8/1/2008–7/31/2010. This project is part of a 3-year integrated project to study generalized opportunistic communications. Our investigation is divided into three phases which was carried out in the past three academic years. In the first year, we focus on analyzing the effect of spectrum sensing error on the performance of a cognitive spread spectrum system. The sensing error may caused by unintentional interference, jamming or simply geographic location difference between a transmitter and its intend receiver. For the last two years we consider more on the spectrum management aspect. As we interpret "spectrum" in the most generalized sense so that it includes all sorts of signal degrees of freedom, i.e., time, bandwidth, space, with the each domain or degree of freedom distributed among different system users. Such an interpretation allow a user to access other users' unused degrees of freedom for transmitting its data. With the generalized spectrum or network resource in mind, we set out for solving the joint relay selection and power/subcarriers allocation problem in a relay-based cooperative OFDMA (orthogonal frequency division multiple access) communication network in the second year. We consider a multiuser MIMO (multiple-input, multiple output) scenario and investigate the joint spatial mode and power distribution issue in the final year. We first study the single-carrier case and then extend to the multi-carrier case.

Since the works done in the first two years has been reported before, we just summarized the main results in Chapters 2 and 3. The third year's effort was devoted to the study of the resource allocation problem in MIMO and MIMO-OFDMA systems, respectively. The main design issue we try to solve is the followings. Given the users' rate requirements of a MIMO-OFDMA system, how to apportion the transmission resources in space, frequency, and user domains so that the total transmit power and each user's average bit error rate are minimized. We consider a orthogonal precoding scheme

based on singular value decomposition (SVD) to begin with. In the orthogonal spatial mode design we construct orthogonal eigenchannels by performing linear operations on the channel matrix's singular vectors under the channel rank constraint. To improve spectral efficiency, we then remove the rank constraint on the number of users allowed on a subcarrier (non-orthogonal design). Although the resulting co-channel interference may cause performance degradation, it is more than compensated for by the increased capacity through a proper resource allocation plan that ensure the associated signal-to-interference ratios are within the tolerable limits. The proposed resource allocation algorithms for both precoding scenarios are designed to minimize the total transmit power while satisfying the users' QoS constraints.

We also examine the resource allocation issue for MIMO systems with limited feedback. More specifically, we consider the codebook based precoding scheme and suggest subcarrier assignment scheme based on the Lagrange multiplier method. For a given subcarrier assignment, we then present a power allocation method which minimizes the average bit error rate performance.

Keyword: Spectrum sensing, resource allocation, MIMO-OFDMA.

Contents

List of Figures

List of Tables

Chapter 1

Introduction

Current spectrum management policy follows a fixed band (channel) assignment scheme which results in inefficient spectrum usage. It was observed [1] that on the average only two percent of the allocated spectrum is actually in use at any given moment and location. Cognitive radio (CR) which allows distributed dynamic spectrum usage was therefore proposed to remedy such a shortcoming in spectrum management.

Based on the CR concept, Chakravarthy *et al.* [1] proposed a dynamic modified direct-sequence spread spectrum (DS-SS) system to which they referred as adaptive waveform communication system (AWCS). Since the spreading sequence of AWCS is synthesized in the transform domain, the system is also called transform domain communication system (TDCS). The basic idea behind TDCS is to generate a spreading sequence whose spectrum avoids existing users or jammers within the SS band.

In most existing works, it is assumed that the channel usage information is perfectly known at transmitter and receiver. In practice, the spectrum conditions at transmitter and receiver are independently estimated at both sides. If the spectrum seen (or measured) by transmitter is different from that seen at receiver, the mismatch between two spreading sequence spectra will cause performance degradation [2]. Spectra mismatches arise because of geographic separation and/or spectrum estimation errors, i.e., either the "true" spectrum represented at two sides are different or the estimated spectra are different although the spectrum representation are the same.

In this subproject, we analyze the effect of spectrum estimation error induced spectrum mismatches on the symbol error rate (SER) performance in additive white Gaussian noise (AWGN) and Rayleigh fading channels, respectively. Notice that TCCS is also a multi-carrier based system and it is expected that this work can be extended to the popular multi-carrier system: orthogonal frequency division multiplexing (OFDM) system.

In the second year, we focus on dynamic resource allocation for relay-based OFDMA systems with fairness considerations. Due to its robustness against frequency selective fading and its flexibility in radio resource allocation for meeting various QoS requirements, the Orthogonal Frequency Division Multiple Access (OFDMA) has been adopted or considered as a candidate multiple access scheme for future wide area broadband wireless networks that support a wide variety of services. OFDMA exploits multi-user diversity in time-varying frequency-selective fading channels by assigning a subcarrier to the MS with the best channel gain [5] and by scheduling the transmission of user data opportunistically.

Recent investigations have shown that if suitable coordination among nodes in a wireless network is in place, a relay-based cooperative communication scheme can significantly improve the performance and extend the coverage range of a wireless link. Capacity and throughput can also be enhanced through proper cooperative resource sharing and scheduling among nodes within a network. Both decode-and-forward (DF) and amplify-and-forward (AF) relaying have been investigated. The choices of the relay scheme and the cooperative nodes often depend on the relative locations of the nodes involved and the corresponding link qualities. AF is a better choice when the topology is such that the received signal-to-noise ratio (SNR) at the relay node is high enough to yield sufficient small decoding error rate and the relay-to-destination link gain is no worse than the source-to-destination gain. The power allocation of OFDM based DF scheme is proposed in [6] where the authors also discusses under what condition(s) a relay should be used. The reception quality and transmission range can be enhanced by incorporating cooperative relays as a transmission option. Motivated by the potential advantages, some multi-hop schemes and their performance gains have been investigated by many and IEEE has formed a task force to develop multi-hop relay specifications for 802.16 air interface.

The problem of resource allocation in conventional OFDMA systems or in relay-aided OFDMA system has been intensively studied. Weighted sum rate maximization (WSRmax) and weighted sum power minimization (WSPmin) problems were considered in [7]. The two optimization problems are solved by employing the Lagrange dual decomposition method. A centralized utility maximization framework was considered in [8]. By introducing a set of pricing variables as weighting factors with the goal of maximizing the utility function of the application layer, the authors solved the optimization of physical-layer transmission strategies (relay strategies and resource allocation) in an efficient manner. Algorithms for subcarriers/time allocation on a relay-based OFDMA system for different frame structures such as time division or frequency division can be found in [9]. Fairness aware adaptive resource allocation in a single-hop OFDM system was considered in [10], [14]. They imposed the proportional fairness constraint to ensure that each user achieve a required date rate. Li and Liu [11] used a graph theoretical approach to solve the resource allocation problem for OFDMA relay networks with fairness constraints on relay nodes by transforming the problem into a linear optimal distribution one.

In this year, we presents low-complexity resource allocation schemes for an OFDMA network with an aim to maximize the overall sum rate with fairness and QoS constraints. We regard sub-carriers, relays and transmission power as part of the radio resource so that the problem of resource allocation becomes that of relay selection and sub-carriers and power assignments. Since this context of the first and second year has been reported before, we only show the main results, simulations and conclusions in chapter 2.

In the final year, the resource allocation problem in MIMO-OFDM systems is considered. A Gram-Schmidt precoding scheme is proposed and this scheme is extended by relaxing the orthogonal constraint. This relaxation makes it possible to improve the spectrum efficiency. However, this scheme requires the complete channel information at transmitter. In practical system, the complete channel information is not available at transmitter because the channel information is feedback through a bandwidth limited feedback channel and should be quantized before sending back. To solve this problem, we also consider a resource allocation problem for MIMO systems with codebook-based precoding.

The rest of this report is organized as followed. Chapter II reviews the results of the first and second year. Then, a resource allocation problem with a Gram-Schmidt precoding scheme (with orthogonal constraint or not) is discussed in chapter III. Finally, a resource allocation problem with codebook-based precoding is investigated to complete our research and we draw a conclusion to end up this report.

Chapter 2

Performance Analysis of Transform Domain Communication Systems in the Presence of Spectral Mismatches

2.1 Introduction to TDCS

The basic idea behind TDCS is to produce a so-called time-domain fundamental modulation waveform (FMW) or a complex spreading sequence which avoids interference from existing users or jammers by dynamically selecting the subcarriers used over a given bandwidth. A block diagram of the TDCS transmitter is illustrated in Fig. 2.1. The transmitter partitions the signal band into N equal-spaced subbands (tones) and performs spectrum estimation to determine which subbands are being used. The spectrum estimator output is an N-dimensional binary vector $\mathbf{A}_x = (A_x(\omega_0), A_x(\omega_1), \cdots, A_x(\omega_{N-1}))$ with $A_x(\omega_i) = 1$ or 0 depending on whether the ith subband is available (1) or not (0). The subscript x will be Tx or Rc to denote if the vector is associated with the transmitter (Tx) or the receiver (Rc). The binary vector $\mathbf{A}_{\mathrm{Tx}}$ is multiplied element-wise by a user-specific random vector $(e^{j\theta(\omega_i)})$ and scaled by constant factor before being inverse discrete Fourier transformed to produce the time-domain FMW. The multiplication of the random vector is to make the FMW noise-like and to provide the multiple access capability. The FMW is used to spread (or as a carrier of) the binary phase shift keying (BPSK) or cyclic code shift keying (CCSK) modulated data sequence.

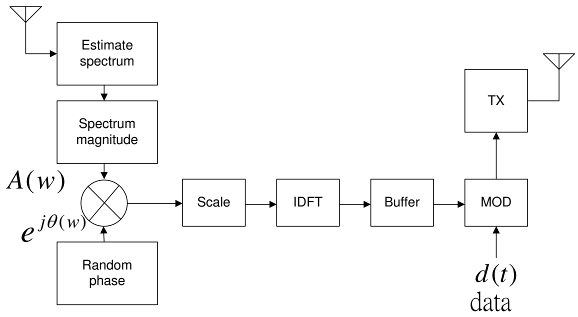

Figure 2.1: Block diagram of the TDCS transmitter

Although TDCS seems to be similar to an OFDM or a multicarrier OFDM system, there are several distinctions between the them. For example, in an OFDM system the number of subcarriers (subbands) is fixed while the number of subbands used in TDCS is dependent on the need or the environment. A detailed comparison can be found in [3].

When the only channel impairment is AWGN, a BPSK-modulated TDCS system with perfect spectrum estimation and matches on both sides of the link yields bit error probability P_e given by

$$P_e = Q\left(\sqrt{\frac{2E_b}{N_0}}\right)$$

where $Q(x) \equiv \frac{1}{\sqrt{2\pi}} \int_x^\infty e^{-y^2/2} dy$.

2.2 Performance Analysis of BPSK-TDCS in AWGN

As defined in previous section, $A_{\mathrm{Tx}}(\omega), A_{\mathrm{Rc}}(\omega)$ are the binary-valued random variables that represent the transmitter's and the receiver's spectrum estimators outputs. $A(\omega)_{\mathrm{Tx}} = 1$ means the transmitter believes ω is available while $A_{\mathrm{Tx}}(\omega) = 0$ implies otherwise. Similar interpretation is attached to $A_{\mathrm{Rc}}(\omega)$.

Depending on the geographic distribution of wireless network users, the true spectra seen from both sides can be identical or different and spectrum mismatches might still arise even if the spectral estimations at both sides are error-free. We refer to such spectra mismatches as network geography induced spectra mismatches. Such mismatches are most likely to occur when the distance between two sides of the link is large. To simplify our analysis we define the true spectrum as such that no existing user is interfered by the transmitted signal and the received waveform is not interfered by any existing user if error-free spectrum estimates are available on both sides of the link.

The true spectrum represented by the binary-valued N-dimensional vector $\mathbf{A} = (A(\omega_0), A(\omega_1), \cdots, A(\omega_{N-1}))$, where N is the size of inverse discrete fourier transform (IDFT), is thus related to the error-free spectrum estimates $\mathbf{A}^o_{\mathrm{Tx}}$ and $\mathbf{A}^o_{\mathrm{Rc}}$ via $\mathbf{A} = \mathbf{A}^o_{Tx} \wedge \mathbf{A}^o_{Rc}$, where $\wedge$ denotes component-wise logical "and" operation.

We assume that $A(\omega_i) = 0$ with probability $1 - P_{sa}$ and $A(\omega_i) = 1$ with probability P_{sa}. Obviously, eight possible scenarios may occur, as listed in Table 2.1. For Cases 1, and 3, interference from existing users is present. In Cases 1 and 5, (additional) noise within the subband ω will be received. The received signal energy is reduced in Cases 2 and 6.

Table 2.1: Eight possible scenarios for a TDCS link.

Case	$(A(\omega), A(\omega)_{\mathrm{Tx}}, A(\omega)_{\mathrm{Rc}})$	The effect of non-ideal match
0	$(0, 0, 0)$	None
1	$(0, 0, 1)$	additional noise and interference are introduced in the subband ω
2	$(0, 1, 0)$	introduce interference to an existing user and reduce the received signal energy
3	$(0, 1, 1)$	introduce interference to an existing user and interference from existing user to the receiver
4	$(1, 0, 0)$	None
5	$(1, 0, 1)$	additional noise in the subband ω is introduced
6	$(1, 1, 0)$	received signal energy is reduced
7	$(1, 1, 1)$	None

If the spectrum estimation is performed in a per-channel manner and each channel is

$$
\begin{aligned}
P_s = & \sum_{N_1=0}^{N}\sum_{i=0}^{N_1}\sum_{j=0}^{N-N_1}\sum_{k_1=0}^{i}\sum_{l_1=0}^{j}\sum_{k_2=0}^{N_1-i}\sum_{l_2=0}^{N-N_1-j}\binom{N}{N_1}P_{sa}^{N_1}(1-P_{sa})^{N-N_1} \\
& \binom{N_1}{i}P_{t0}^{i}(1-P_{t0})^{N1-i}\binom{N-N_1}{j}P_{t1}^{N-N_1-j}(1-P_{t1})^{j}\binom{i}{k_1}P_{r0}^{k_1}(1-P_{r0})^{i-k_1} \\
& \binom{N_1-i}{k_2}P_{r0}^{k_2}(1-P_{r0})^{N_1-i-k_2}\binom{j}{l_1}P_{r1}^{j-l_1}(1-P_{r1})^{l_1}\binom{N-N_1-j}{l_2} \\
& P_{r1}^{N-N_1-j-l_2}(1-P_{r1})^{l_2}P_e\left(\frac{E_s(\frac{k_1+l_1}{\max(i+j,1)})}{N_0(1+\frac{k_2+l_2}{\max(k_1+l_1,1)})+\frac{l_1+l_2}{\max(k_1+l_1,1)}N_I}\right) \qquad (2.15)
\end{aligned}
$$

independently used, then it is reasonable to assume that the following four probabilities,

$$
\begin{aligned}
P_{t0} &= \mathrm{P}_r\{A_{\mathrm{Tx}}(\omega)=1|A(\omega)=1\} \\
P_{t1} &= \mathrm{P}_r\{A_{\mathrm{Tx}}(\omega)=0|A(\omega)=0\} \\
P_{r0} &= \mathrm{P}_r\{A_{\mathrm{Rc}}(\omega)=1|A(\omega)=1\} \\
P_{r1} &= \mathrm{P}_r\{A_{\mathrm{Rc}}(\omega)=0|A(\omega)=0\},
\end{aligned}
$$

and their complementary probabilities are independent of ω_i.

The above assumptions imply that $\mathbf{A}$ is binomial distributed with parameter P_{sa} and furthermore, $\mathbf{A}_{\mathrm{Tx}}$ and $\mathbf{A}_{\mathrm{Rc}}$ are obtained by modifying $\mathbf{A}$ based on P_{t0} (P_{r0}) and P_{t1} (P_{r1}), respectively.

It can be proved that in a AWGN/Rayleigh fading channel with one-sided power spectral density of N_0 W/Hz, the bit error rate (BER) expression is given by (2.15). where P_e is summarized in Table 2.2.

The error floor becomes

$$
\begin{aligned}
P_s = C\,[P_{sa}(1-P_{t0}P_{r0})+ \\
(1-P_{sa})(P_{t1}+P_{r1}-P_{t1}P_{r1})]^N \qquad (2.16)
\end{aligned}
$$

where C is a parameter depending on modulation type. The exact value of C is tabulated in table 2.3.

Table 2.2: P_e in AWGN

$P_e(x)$	Modulation Type
$Q(2\sqrt{x})$	BPSK
$1-[1-Q(\sqrt{x})]^2$	QPSK
$\frac{1}{\pi}\int_0^{\frac{(M-1)\pi}{M}} \exp\left[\frac{-\sin^2(\pi/M)x}{\sin^2\phi}\right]d\phi$	MPSK
$\frac{2(M-1)}{M}Q\left(\sqrt{\frac{6x}{M^2-1}}\right)$	MPAM
$1-\left(1-\frac{2(\sqrt{M}-1)}{\sqrt{M}}Q\left(\sqrt{\frac{3x}{M-1}}\right)\right)^2$	MQAM

Table 2.3: C in AWGN channel

C	Modulation Type
$\frac{1}{2}$	BPSK
$\frac{3}{4}$	QPSK
$\frac{M-1}{M}$	MPSK
$\frac{M-1}{M}$	MPAM
$1-\left(1-\frac{\sqrt{M}-1}{\sqrt{M}}\right)^2$	MQAM

For flat Rayleigh fading channels, the average probability of symbol error can be shown to be given by $\overline{P_s} = \int_0^\infty P_s(x)p_{r_s}(x)dx$, where $P_s(x)$ is the probability of symbol error in AWGN with SNR x,

$$p_{r_s}(x) = \frac{1}{\overline{r}_s}e^{-\frac{x}{\overline{r}_s}}$$

and $\overline{r}_s$ is the average SNR per symbol. From [4], the average probability of symbol error is almost the same as (2.15) except for P_e. The modified P_e is given in table 2.4, where $g_{\text{PSK}} = \sin^2\frac{\pi}{M}$. Notice that coherence here means the receiver has perfect channel state information (CSI), e.g., the amplitude attenuation, phase influence, and delay time are known at receiver.

Notice that the extension to other fading channel is straightforward. For example, if the channel is Nakagami-m, the symbol error rates for MPAM modulation type can be

Table 2.4: P_e in flat Rayleigh channel, where $g_{\text{PSK}} = \sin^2 \frac{\pi}{M}$

$P_e(x)$	Modulation Type
$\frac{1}{2}\left(1 - \sqrt{\frac{x}{1+x}}\right)$	BPSK
$\left(\frac{M-1}{M}\right)\left\{1 - \sqrt{\frac{g_{\text{PSK}}x}{1+g_{\text{PSK}}x}}\frac{M}{(M-1)\pi}\left[\frac{\pi}{2} + \arctan\left(\frac{g_{\text{PSK}}x}{1+g_{\text{PSK}}x}\cot\frac{\pi}{M}\right)\right]\right\}$	MPSK
$\frac{(M-1)}{M}\left(1 - \sqrt{\frac{3x}{M^2-1+3x}}\right)$	MPAM
$2\left(\frac{\sqrt{M}-1}{\sqrt{M}}\right)\left(1 - \sqrt{\frac{1.5x}{M-1+1.5x}}\right) - \left(\frac{\sqrt{M}-1}{\sqrt{M}}\right)^2$ $\left(1 - \sqrt{\frac{1.5x}{M-1+1.5x}}\left(\frac{4}{\pi}\arctan\sqrt{\frac{M-1+1.5x}{1.5x}}\right)\right)$	MQAM

obtained by substituting $P_s(x)$ with

$$P_s(x) = \left(\frac{M}{M-1}\right)\left[1 - \mu\sum_{k=0}^{m-1}\binom{2k}{k}\left(\frac{1-\mu^2}{4}\right)^k\right]$$

for m is integer and $\mu \equiv \sqrt{\frac{3x}{m(M^2-1)+3x}}$. For m is noninteger,

$$P_s(x) = \left(\frac{M}{M-1}\right)\frac{1}{\sqrt{\pi}}\frac{\sqrt{3x/m(M^2-1)}}{[(m(M^2-1)+3x)/m(M^2-1)]^{m+1/2}} \frac{\Gamma(m+\frac{1}{2})}{\Gamma(m+1)}\,{}_2F_1\left(1, m+\frac{1}{2}; m+1; \frac{m(M^2-1)}{m(M^2-1)+3x}\right)$$

where $\Gamma(\cdot)$ is gamma function and ${}_2F_1(\cdot,\cdot;\cdot;\cdot)$ is the Gauss hyper geometric function.

2.3 Simulation results

In this section, we show that the simulation of the performance of TDCS agrees with (2.15) with $P_{sa} = 0.5$ for different case. The size of IDFT N is set equal to 8.

Example 2.1. *The effect of* P_{t0}

In this example, the effect of P_{t0} *is illustrated in Fig. 2.2. The parameters are set as followed:* $P_{t1} = 0.5$, $P_{r0} = 0.7$, $P_{r1} = 0.4$ *and* $\frac{E_b}{N_I} = 0$ *dB. It is obvious that the simulation result is almost the same to analytic result.*

Example 2.2. *The effect of* P_{r0} *and* P_{r1}

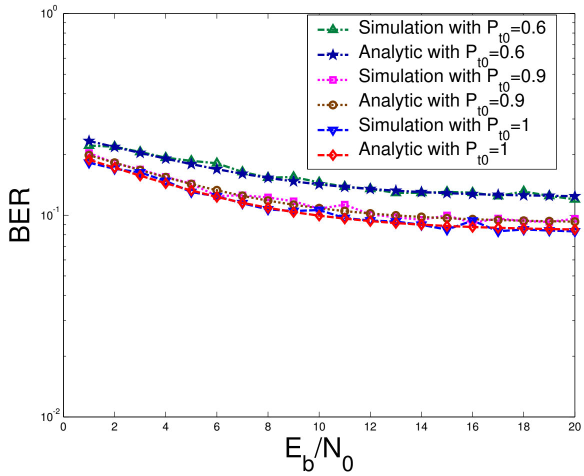

Figure 2.2: BER performance for different P_{t0}

Fig. 2.3 illustrate the simulation result with varying P_{r0} *and* P_{r1} *and show the agreement with analytic result. The other parameters are set as followed:* $P_{t0} = 0.9$, $P_{t1} = 0.5$ *and* $\frac{E_b}{N_I} = 0$ *dB. Notice that the setting of* P_{r0} *and* P_{r1} *is equivalent to assign* $A(\omega)_{Rc} = \begin{cases} 1 & \text{with } P_{r0} \\ 0 & \text{with } P_{r1} = 1 - P_{r0} \end{cases}$*, namely, it is determined by receiver without considering the environment. It may be suggested that the strategy is a good strategy when always assigns* $A(\omega) = 1$ *without estimating the spectrum at receiver.*

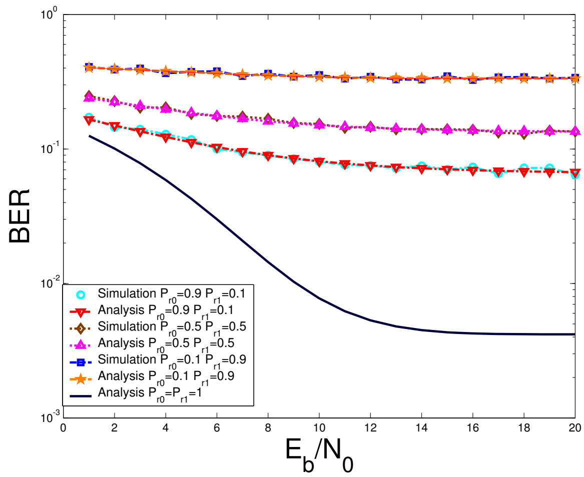

Figure 2.3: BER performance for different P_{r0} and P_{r1}

Example 2.3. ***The effect of*** P_{t1}

The effect of P_{t1} *is illustrated in Fig. 2.4. We can see that they are almost identical. The parameters are set as followed:* $P_{t0} = P_{r0} = P_{r1} = 0.9$ *and* $N_I = 0$ *dB. A interesting thing is that they are intersected for different* P_{t1}*. It can be explained by observing that only* $j = N - N_1$ *has nonzero value in (2.15) if* $P_{t1} = 0$*. Since* $j = N - N_1$, $l_2 = 0$*. This implies it is possible that interference is smaller than other cases at high* $\frac{E_b}{N_0}$*. To illustrate the argument, consider Fig. 2.5. In Fig. 2.5,* $P_{t0} = P_{r0} = 1$*, and* $\frac{E_b}{N_I} = 0$ *dB. When* $P_{r1} = 0.7$*, interference is more serious and centered at higher* l_1 *than that in* $P_{r1} = 0.9$*. For* $P_{t1} = 0$*, it is possible to reduce interference at cost of* E_b*, which can be expected by (2.17).*

$$P_b = \sum_{N_1=0}^{N} \sum_{l_1=0}^{N-N_1} \binom{N}{N_1} \frac{1}{2}^N \binom{N-N_1}{l_1} P_{r1}^{N-N_1-l_1} (1-P_{r1})^{l_1} f \tag{2.17}$$

where $f = \begin{cases} Q\left(\sqrt{\dfrac{2E_b\left(\frac{N_1+l_1}{\max(N,1)}\right)}{\frac{l_1}{\max(N_1+l_1,1)}N_I}}\right), & P_{t1} = 0 \\ Q\left(\sqrt{\dfrac{2E_b\left(\frac{N_1}{\max(N_1,1)}\right)}{\frac{l_1}{\max(N_1,1)}N_I}}\right), & P_{t1} = 1 \end{cases}$

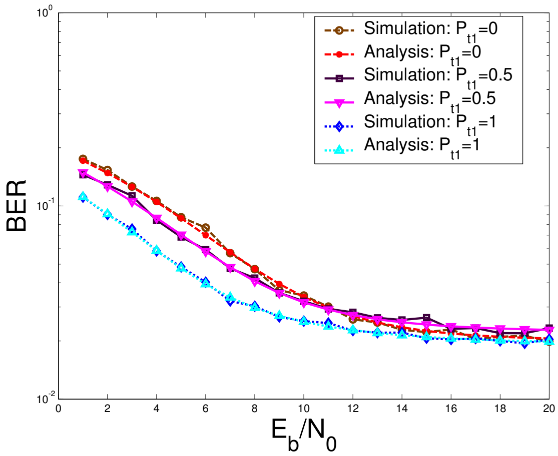

Figure 2.4: BER performance for different P_{t1}'s

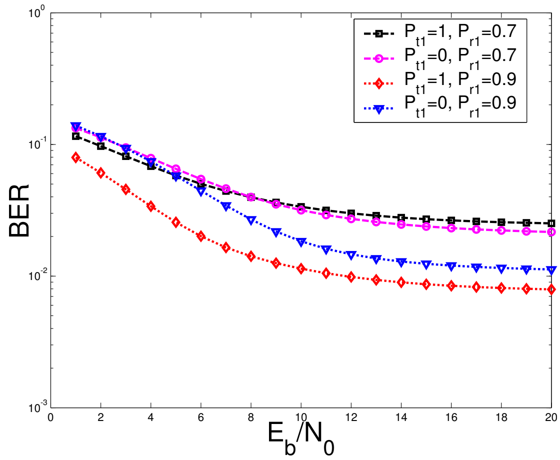

Figure 2.5: The effect of interference

2.4 Chapter Summary

CR has attracted much interest because of its potential to greatly enhance the spectrum utilization efficiency. TDCS is a novel new candidate SS technique that invokes the CR concept. In the first year, we consider the effect of spectra mismatches due to spectral estimation error. BER expressions for BPSK signals in various operating conditions are given. We also derive analytical SER expressions for other modulations like MPSK, QAM signals and flat Rayleigh fading channels. Our analysis can easily be extended to other flat-fading channels by deriving the corresponding $P_s(x)$. It is shown that the spectral estimation error results in error floor. As expected, the BER/SER performance is improved and the error floor is reduced when the per-tone (single-subcarrier) detection error decrease. Increasing the number of subcarriers (processing gain) in the SS band also has similar effect. Based on this, it suggests that the best access police is to choice all subbands in terms of BER/SER if the subbands are estimated as idle state. We also find that the BER/SER performance is more sensitive to the spectral estimation error at the receiver than that at the transmitter.

There are quite a few issues that remain to be solved. Firstly, we use a simple Bernoulli distribution to model the estimation error, which is appropriate if the spectral estimation is carried out in a tone-by-tone manner. A more realistic model depends on the spectral estimation method used. It would be interesting to see how the system behaves under different spectral mismatch models. Secondly, a soft decorrelation process might be useful to reduce the impact of spectral mismatches and enhance system performance. Furthermore, cooperative spectrum sensing and prediction should be considered in the future to decrease the mismatch probability. Finally, it is both natural and desirable to extend the transceiver techniques and the associated spectral model to a multiple access scenario with guaranteed performance.

Chapter 3

Dynamic Resource Allocation for Relay-based OFDMA Systems with Fairness Considerations

3.1 System Model

We consider an N-subcarrier OFDMA system in which there is a BS, M fixed relay nodes, and K MS' randomly distributed within a cell. Assume that uplink channel state information is perfectly known to the BS which also knows the minimum rate and QoS (bit error rate) requirements of the MSs. The BS, acts as a central control device, will carry out all resource allocation operations, including collecting link information, appropriating resources, and informing MS' about their assigned resources. Similar to the conventional relay-based cooperative communication systems, we assume a two-phase (time-slot) transmission scheme with perfect timing synchronization among all network users. Each subcarrier suffers from slow Rayleigh fading so that there is no change of the channel state during a two-phase period. A data stream from a source user must be carried by the same subcarrier no matter it is transmitted by a source node or a relay node.

The transmission pattern is half-duplex such that a MS transmits while the relay and the BS listen (receive) in the first time slot. In the second phase, the relay stations transmit to the BS while the source MS' send new data packets via direct links without relaying. This transmission protocol was discussed in [12] and was shown to be more throughput-efficient than the conventional protocol with which a source MS remains idle in the second phase. Only the decode-and-forward (DF) cooperative relay scheme is considered and the maximum-ratio-combining detector is employed by the destination (BS) node, assuming perfect decoding at the relays.

3.2 Problem Formulation

Let us denote by $h_{SD}(n,k)$ the fading coefficient (gain) for the channel (link) between the kth source MS and the BS on the subcarrier n, by $h_{RD}(n,m)$, the fading coefficient for the channel between the mth relay and the BS on the subcarrier n, and by $h_{SR_m}(n,k)$, the fading gain for the channel between MS k and relay m on subcarrier n. The corresponding transmit powers and received signals are denoted by $P_S(n,k)$, $P_R(n,m)$, $P_{SR_m}(n,k)$ and $y_{SD}(n,k)$, $y_{RD}(n,k)$, $y_{SR_m}(n,k)$, respectively. During any given phase we have for the source-to-destination (SD) link

$$y_{SD}(n,k) = h_{SD}(n,k)x_k + n(n,k) \tag{3.1}$$

where x_k represents the data sent by the kth MS and $n(n,k)$ is the additive Gaussian noise for the corresponding link. The associated achievable rate in bits/sec/Hz is given by

$$R_{SD}(n,k) = \log_2\left[1 + \frac{P_S(n,k)|h_{SD}(n,k)|^2}{\Gamma\sigma^2}\right] \tag{3.2}$$

where $\Gamma \simeq -\ln(5{*}\mathrm{BER})/1.5$ is the signal-to-noise ratio (SNR) gap related to the designed BER [13]. The inclusion of Γ in (3.2) (and other related rate-power equations appear in subsequent discourse) has implicitly imposed the user's QoS requirement. Rearranging (3.2) yields

$$P_S(n,k) = \left(2^{R_{SD}(n,k)} - 1\right)\frac{\Gamma\sigma^2}{|h_{SD}(n,k)|^2}. \tag{3.3}$$

Since we allow a source (MS) node to be active for both phases, a fair comparison on the achievable rate should be measured in a per time slot basis, or with respect to the total consumed energy. For convenience, we shall normalize a time slot to one so that henceforth the consumed energy is equivalent to the consumed power. Because the channel states are assumed to remain the same during any two time-slot period, the power allocated to the direct link on each time slot should be the same. The power (consumed energy) for two OFDM symbols can thus be expressed as

$$P_D(n,k) = 2\left(2^{R(n,k)/2} - 1\right)\frac{\Gamma\sigma^2}{|h_{SD}(n,k)|^2} \tag{3.4}$$

where $P_D(n,k)$ is the power needed for the direct link, and $R(n,k)$ is the rate achievable by the system for a duration of two symbol intervals. Similarly, the signal carried by the nth subcarrier and received by the mth relay for the kth MS is given by

$$y_{SR_m}(n,k) = h_{SR_m}(n,k)x_k + n(n,k). \tag{3.5}$$

In the first phase, the kth MS sends x_k to the mth relay with a achievable rate of

$$R_{SR_m}(n,k) = \log_2\left[1 + \frac{P_{SR_m}(n,k)|h_{SR_m}(n,k)|^2}{\Gamma\sigma^2}\right] \tag{3.6}$$

or equivalently, this source-to-relay (SR) link rate can only be achieved if the source power is greater than or equal to

$$P_{SR_m}(n,k) = \left(2^{R_{SR_m}(n,k)} - 1\right)\frac{\Gamma\sigma^2}{|h_{SR_m}(n,k)|^2}. \tag{3.7}$$

Relay nodes transmit the data packet to destination in the second phase. The destination node receives two scaled packets containing the same data stream and combines them by the maximum-ratio-combining (MRC) scheme. The achievable MRC rate of the kth user on subcarrier n with the help of perfectly decoding relay m is

$$R_{R_m}(n,k) = \log_2 \left[1 + \frac{P_{SR_m}(n,k)|h_{SD}(n,k)|^2 + P_R(n,m)|h_{RD}(n,m)|^2}{\Gamma\sigma^2}\right] \tag{3.8}$$

The corresponding minimum required relay power is thus given by

$$P_R(n,m) = \frac{(2^{R_{R_m}(n,k)} - 1)\Gamma\sigma^2 - P_{SR_m}(n,k)|h_{SD}(n,k)|^2}{|h_{RD}(n,m)|^2} \tag{3.9}$$

The total power $P_{R_m}(n,k) \stackrel{def}{=} P_{SR_m}(n,k) + P_R(n,m)$ for the composite direct-plus-relay m link is

$$P_{R_m}(n,k) = \left(2^{R_{R_m}(n,k)} - 1\right)\Gamma\sigma_n^2 \left[\tfrac{1}{|h_{SR_m}(n,k)|^2} + \tfrac{1}{|h_{RD}(n,m)|^2} - \tfrac{|h_{SD}(n,k)|^2}{|h_{SR_m}(n,k)|^2 |h_{RD}(n,m)|^2}\right] \tag{3.10}$$

Define the link power gains, $g_D(n,k)$, $g_{SR}(n,k)$, $g_{RD}(n,k)$, and $g_{R_m}(n,k)$, for the direct, component and the composite links by

$$\begin{aligned} g_D(n,k) &= |h_{SD}(n,k)|^2 \\ g_{SR_m}(n,k) &= |h_{SR_m}(n,k)|^2 \\ g_{R_mD}(n,k) &= |h_{R_mD}(n,k)|^2 \end{aligned} \tag{3.11}$$

and

$$g_{R_m}(n,k) = \frac{g_{SR_m}(n,k) g_{R_mD}(n,k)}{g_{R_mD}(n,k) + g_{SR_m}(n,k) - g_D(n,k)} \tag{3.12}$$

and the corresponding link gain-to-noise ratios (GNRs) by

$$\begin{aligned} \alpha_D(n,k) = \frac{g_D(n,k)}{\Gamma\sigma_n^2},\ \alpha_{SR_m}(n,k) = \frac{g_{SR_m}(n,k)}{\Gamma\sigma_n^2} \\ \alpha_{R_mD}(n,k) = \frac{g_{R_mD}(n,k)}{\Gamma\sigma_n^2},\ \alpha_{R_m}(n,k) = \frac{h_{R_m}(n,k)}{\Gamma\sigma_n^2} \end{aligned} \tag{3.13}$$

for all n and k. Using the above notations, we can express the achievable rate for the relayed link as

$$R(n,k) = \min\left\{R_{SR_m}(n,k), R_{R_m}(n,k)\right\} \tag{3.14}$$

The optimal power allocation is such that $R_{SR_m}(n,k) = R_{R_m}(n,k)$, which implies the power ratio

$$\frac{P_R(n,m)}{P_{SR_m}(n,k)} = \frac{g_{SR_m}(n,k) - g_D(n,k)}{g_{R_mD}(n,k)} \tag{3.15}$$

For the conventional DF scheme, cooperative relay is beneficial if it offers a higher achievable rate with the same power or, equivalently, the composite link should require less power to obtain the same achievable rate. (3.2), (3.6) and (3.8) imply that this happens iff

$$\begin{aligned} g_{R_mD}(n,k) &> g_D(n,k) \\ \max_m g_{SR_m}(n,k) &> g_D(n,k) \end{aligned} \tag{3.16}$$

The above conditions are necessary but not sufficient for the DF scheme under consideration, which gives another necessary condition

$$g_{R_m}(n,k) > g_D(n,k) \tag{3.17}$$

or, if multiple relay nodes are available

$$\max_m g_{R_m}(n,k) \overset{def}{=} g_R(n,k) > g_D(n,k) \tag{3.18}$$

i.e., at least one of the candidate composite link should have a link gain greater than that of the direct (SD) link. Assuming the optimal power ratio (3.15), we can show that a necessary and sufficient condition for a single-relay system is

$$\frac{g_{SR_m} - g_D}{g_{SR_m} + g_{R_mD} - g_D} \frac{g_{R_mD} - g_D}{g_D^2} = \frac{g_{R_m} - g_D}{g_D^2} > \gamma \tag{3.19}$$

where $\gamma = \frac{P_D(n,k)}{4\Gamma\sigma^2}$ and the link gains' dependence on the pair (n,k) is omitted for the sake of brevity. For multiple-relay systems, (3.19) becomes

$$\max_m \frac{g_{R_m} - g_D}{g_D^2} \overset{def}{=} \max_m G_m > \gamma \tag{3.20}$$

It verifiable that the conditions (3.18) and (3.20) are equivalent if $P_D(n,k)\alpha_D(n,k)/2 \ll 1$.

The achievable sum rate of the system over a two-symbol interval for a subcarrier/power allocation is thus given by

$$\begin{aligned} R = \\ \sum_{k=1}^{K} \Bigg\{ \sum_{n \in S_R} \rho_{nk} \log\left[1 + P_{R_{m(n,k)}}(n,k)\alpha_{R_{m(n,k)}}(n,k)\right] \\ + \sum_{n \in S_D} 2\rho_{nk} \log\left[1 + P_D(n,k)\alpha_D(n,k)/2\right] \Bigg\} \end{aligned} \tag{3.21}$$

where S_R and S_D are the sets of relayed and un-relayed subcarriers, and $m(n,k)$ denotes the relay node used for the subcarrier (n,k). ρ_{nk} is the binary valued indicator function which signifies if subcarrier n is allocated to MS k and is nonzero and equal to one only if the latter condition is valid. Following [14] we define the fairness index, F, as

$$F = \frac{\left(\sum_{k=1}^{K} \frac{R_k}{R_{k,min}}\right)^2}{K \sum_{k=1}^{K} \left(\frac{R_k}{R_{k,min}}\right)^2} \tag{3.22}$$

where $R_{k,min}$ is the minimum required rate for MS k and R_k is the achievable rate computed by (3.21) for a given subcarrier/power allocation. With the above definitions and derived relations, we formulate the resource allocation problem as the vector (multi-criteria) optimization problem

$$\text{maximize } [R, F]^T \tag{3.23}$$

subject to

$$\sum_{n \in S_R} \rho_{n,k} \log\left[1 + P_{R_m}(n,k)\alpha_{R_m}(n,k)\right] + \sum_{n \in S_D} 2\rho_{n,k} \log\left[1 + P_D(n,k)\alpha_D(n,k)/2\right] \geq R_{k,min}, \quad \forall\ k \tag{3.24}$$

$$\sum_{k=1}^{K} \rho_{n,k} = 1, \quad \rho_{n,k} \in \{0,1\} \quad \forall\ k, n \tag{3.25}$$

$$\sum_{k=1}^{K} \left[\sum_{n \in S_R} P_{R_m}(n,k) + \sum_{n \in S_D} P_D(n,k)\right] = P_T$$
$$P_D(n,k) \geq 0, \quad P_{R_m}(n,k) \geq 0, \quad \forall\ k, n \tag{3.26}$$

Constraint (3.24) guarantees that the minimum rate requirements $R_{k,min}$ are met. Constraint (3.25) implies that a subcarrier serves only one user such that there is no inter-subcarrier interference. The total transmit power of the BS and relay nodes is limited by the constraint (3.26). The object of assigning subcarriers and relays to all MS users with a proper power distribution to maximize the sum rate and fairness index is a mixed integer programming problem. Instead of trying to find a polynomial-time optimal solution (which is very difficult if not impossible), we propose low-complexity suboptimal algorithms that offer near-optimal performance for the problem in hand.

3.3 Proposed algorithms

Two suboptimal algorithms to solve the above resource allocation problem (3.24)-(3.26) are presented in this section. For convenience, we refer to these two algorithms as Algorithms A and B, respectively. Algorithm A consists of four steps while the other algorithm (Algorithm B) has three steps only. Steps 2 and 3 for both algorithms are the same. The difference between the two algorithms is the first step. The last step of Algorithm A is to fine-tune the relay allocation. Each source node can have multiple cooperative relay nodes which are determined in a per-subcarrier basis. However, each subcarrier is limited to have at most one relay node but the local optimal relay node (for a particular subcarrier) is always selected for cooperative DF transmission. The Algorithms A and B are summary in Table 3.1 and 3.2, respectively and the principle of design can be found in the previous report.

3.4 Numerical Results and Discussions

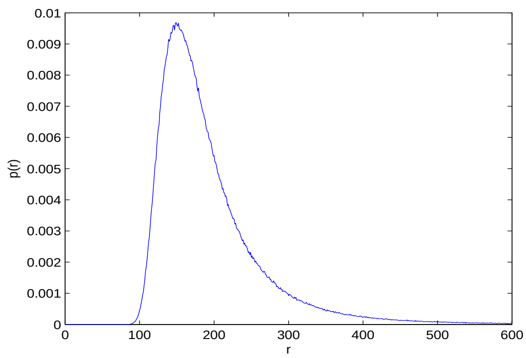

Figure 3.1: The probability density function of the user location distribution; $r_0 = 150$ m.

Numerical performance of the proposed algorithms is presented in this section. We consider a network with four MS nodes that are randomly distributed within a 120-degree section of a 600-meter radius circle centered at the BS. The relay stations are

Table 3.1: Algorithm A

Step 1:	**for** $n = 1{:}\ N$
	for $k = 1{:}\ K$
	if $g_{R_m}(n,k) > g_D(n,k)$
	$m = \arg\max_\ell g_{R_l}(n,k)$
	else
	$m = 0$
	end
	Compute $g_{ELG}(n,k)$
	end
	end
Step 2:	Decide the assignment order n'
	for $n' = 1{:}\ N$
	Compute $\Delta(n'k)$
	$k^* = \arg\max_k(\Delta(n',k))$
	$N_{k^*} \leftarrow N_{k*} \cup \{n'\}$
	end
Step 3:	**for** $k = 1{:}\ K$
	while$(R_k < R_{k,min})$
	$k^* = \arg\max_k(R_k - R_{k,min})$
	$n' = \arg\min_n g_{ELG}(n,k)\ ,\ n \in N_{k^*}$
	$N_k \leftarrow N_k \cup \{n'\} \quad N_{k^*} \leftarrow N_{k^*} \setminus \{n'\}$
	end
	end
Step 4:	Check each relayed subcarrier.
	Compute $g_{ELG}(n,k)$ and make necessary link switches.
	Calculate R and F.

placed on a circle with a 200-meter radius with a equal angular spacing. The probability density function (pdf) of the MS locations is given by [15]

$$P = \frac{r_0^4}{r^5} \exp\left[-\frac{5}{4}\left(\frac{r_0}{r}\right)^4\right]. \tag{3.27}$$

where $r > 0$ is the radius. The pdf with $r_0 = 150$ m is plotted in Fig. 3.1. Each transmitted signal experiences attenuation with a path loss exponent value of 3.5 and, in any direct or relay link, each subcarrier suffers from independent Rayleigh fading. For the convenience of comparison, we normalized the link gain with respect to the worst-case gain corresponding to the longest link distance. We set $\sigma_n^2 = 1$. 4×10^5 simulation

Table 3.2: Algorithm B

Step 1:	**for** $n = 1{:}\ N$
	for $k = 1{:}\ K$
	if $G_m(n,k) > \frac{P_T}{4N\Gamma\sigma^2}$
	$m = \arg\max_\ell G_\ell(n,k)$
	else
	$m = 0$
	end
	Compute $g_{ELG}(n,k)$
	end
	end
Step 2:	Decide the assignment order n'
	for $n' = 1{:}\ N$
	Compute $\Delta(n'k)$
	$k^* = \arg\max_k(\Delta(n',k))$
	$N_{k^*} \leftarrow N_{k*} \cup \{n'\}$
	end
Step 3:	**for** $k = 1{:}\ K$
	while$(R_k < R_{k,min})$
	$k^* = \arg\max_k(R_k - R_{k,min})$
	$n' = \arg\min_n g_{ELG}(n,k)\ ,\ n \in N_{k^*}$
	$N_k \leftarrow N_k \cup \{n'\} \quad N_{k^*} \leftarrow N_{k^*} \setminus \{n'\}$
	end
	end

runs were carried out to estimate the performance. We compare the sum rate and fairness performance of our algorithms with that of the Awad-Shen (AS) algorithm [16]. Because the AS algorithm considers amplify-and-forward cooperative relay and allow each source to use at most one relay node, we modify it so that the comparison with ours is as fair as possible. The modified AS algorithm is listed in Table 3.3.

In Fig. 3.2 and Fig. 3.3 we compare the performance of our algorithms that of the optimal sum rate algorithm and the algorithm in [16]. We assume that the system has 2 MSs and 3 relay nodes. The number of subcarriers are 8, the total power is 80 and the required BER is 0.001. We find that our algorithms achieve about 94% of the optimal sum rate and the fairness index is significant better than that achievable by the optimal sum rate algorithm. This is because the latter does not consider the fairness index and

Table 3.3: The Modified Awad-Shen Algorithm

Satisfy sources' rate requirements
while $K \neq \emptyset$ **do**
  $n \leftarrow random(N)$
  $k^* = \arg_k \max R(k,n)$
  $N_{k^*} \leftarrow N_{k*} \cup \{n\} \quad N \leftarrow N \setminus \{n\}$
  $R^{k^*} = R^{k^*} + R(k^*, n)$
  while $R^{k^*} < R_{k,min}$ **do**
    $n^* = \arg_n \max R(k^*, n)$
    $N_{k^*} \leftarrow N_{k*} \cup \{n^*\} \quad N \leftarrow N \setminus \{n^*\}$
    $R^{k^*} = R^{k^*} + R(k^*, n^*)$
  end while
  $N \leftarrow N \setminus N_{k^*} \quad K \leftarrow K \setminus \{k^*\}$
end while
Allocate remaining subcarrier
while $N \neq \emptyset$ **do**
  $k^* = \arg_k \max R(k,n)$
  $N_{k^*} \leftarrow N_{k*} \cup \{n\} \quad N \leftarrow N \setminus \{n\}$
end while

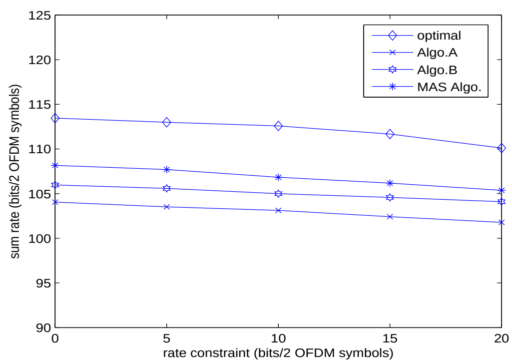

Figure 3.2: Comparison of the sum rate performance for the proposed algorithms and the AS algorithm; 2 MSs, 3 relay nodes, $N = 8$, $P_T = 80$, BER = 0.001.

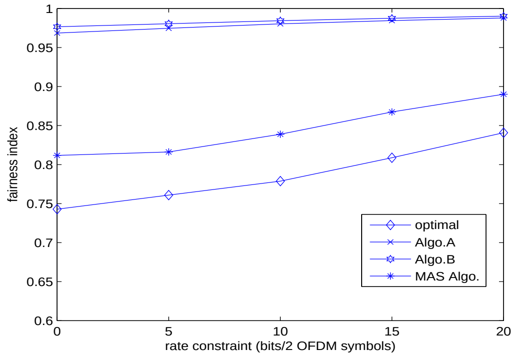

Figure 3.3: Comparison of the fairness performance for the proposed algorithms and the AS algorithm; 2 MSs, 3 relay nodes, $N = 8$, $P_T = 80$, BER $= 0.001$.

is designed to maximize sum rate performance only. The sum rate performance of that presented in [16] is about 1% higher than ours while our fairness index is much better. In Figs. 3.4 and 3.5, we consider the case when there are 4 MSs, 3 relay nodes and the system uses 128 subcarriers with a maximum total power of 128 and 0.001 BER requirement. Again, compared with our algorithms, the sum rate of [16] is about 1% higher while suffers from 30% loss of fairness performance. 3.3 and 3.5 indicate that our fairness index is robust against the system parameters variation but the algorithm of [16] is not. Our algorithms have another advantage against the AS algorithm 3.4, i.e., when the minimum rate requirements are 80 (bits), our algorithms are capable of providing an allocation solution such that all MS rate requirements are met while the AS algorithm fails to do so. Algorithm B outperforms Algorithm A since the latter suffers from a little performance loss in step one. Algorithm B achieves a better performance at the expense of higher computation complexity though. In short, both proposed algorithms offer a satisfactory balance between maximizing the sum rate and the fairness performance.

3.5 Chapter Summary

Cooperative relays provide additional transmission opportunities and offer the potential to improve overall system capacity, throughput and the coverage range of a BS. It is thus

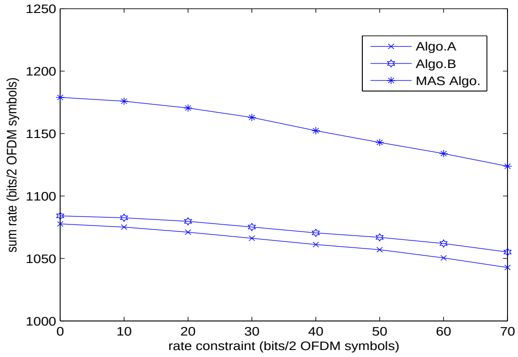

Figure 3.4: Sum rate performance of the proposed algorithms and the AS algorithm; 4 MSs, 3 relay nodes, $N = 128$, $P_T = 128$, BER $= 0.001$.

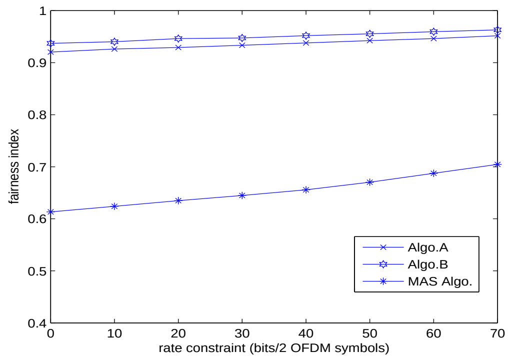

Figure 3.5: Fairness performance of the proposed algorithms and the AS algorithm; 4 MSs, 3 relay nodes, $N = 128$, $P_T = 128$, BER $= 0.001$.

natural to regard relay stations as part of the network radio resource and their allocation should be considered in conjunction with other conventional radio resources to optimize the system performance. We have proposed two algorithms that maximize the sum rate and fairness while meeting the individual user's minimum rate requirement. No optimal solution to the problem discussed here is known, and our computational complexity is much less than exhaustive search. Numerical results indicate that our low-complexity algorithms not only achieve 94% of the optimal sum rate but also provide very robust fairness no matter what the minimum rate constraints are. The proposed algorithms also provide powerful allocation to meet the highly minimum rate constraints for all users.

Chapter 4

Resource Allocation for Orthogonally Precoded MIMO Systems

4.1 Background

In recent years, the MIMO technology has drawn intensive attention since it promises a capacity that is proportional to the smallest number of antennas used at the transmit and the receive sites [29]. Many novel MIMO transceiver designs have been proposed and verified in past decade. In [30], the BLAST (Bell Labs Layered Space-Time) architectures proposed exploits the capacity advantage of multiple antenna systems for multiplexing. A simple but ingenious transmit diversity technique-the Alamouti scheme [31], is designed to achieve diversity gain and has been adopted in the standards of many communication systems. In addition, SVD also can be used in MIMO systems as the beam patterns of the beamforming technology to improve the system performance. Some SVD based orthogonalization schemes have been proposed [32]-[33] for MIMO precoding such that the co-channel interference (CCI) can be minimized. A basic assumption used is that there exits enough orthogonal spatial channels that each user will have access to at least one of them, which, unfortunately, may not always be valid. Besides SVD based precoding, there are also other precoding schemes such as lattice-reduction based precoding [34] or codebook based precoding [27]-[28]. In the design of our precoding scheme, we use the SVD to obtain the basis of the precoding vectors.

4.2 System Parameters and Transceiver Model

Consider a MIMO-OFDMA system with a single base station (BS) equipped with T_x antennas and K mobile station (MS) users, each equipped with R_x antennas. The frequency band used contains M subcarriers which are to be allocated to the K MS'. Besides orthogonal subcarriers, such a system provides additional spatial channels for transmission.

Let the kth MS' channel matrix for subcarrier m be denoted by the $R_x \times T_x$ matrix $\mathbf{H}_{mk}$. Applying SVD to $\mathbf{H}_{mk}$ gives

$$\mathbf{H}_{mk} = \mathbf{U}_{mk}\boldsymbol{\Lambda}_{mk}\mathbf{V}_{mk}^{\dagger} \tag{4.1}$$

where $\mathbf{U}_{mk}$ contains the left singular vectors of $\mathbf{H}_{mk}$ and $\mathbf{U}_{m,k}$ contains the right singular vectors of $\mathbf{H}_{mk}$. $\boldsymbol{\Lambda}_{mk}$ is the diagonal matrix with diagonal entries being the singular values (SVs). In order to separate the signals from different user perfectly the proposed scheme provides at most R eigen-channels on the same subcarrier where R is the rank of the MIMO channel matrix. (Here we assume that the channel matrices of all users are all full rank. Although there are still the case that the channel matrix may be rank-deficient due to the spatial correlation, we can still suppose the channel matrix be full rank with some negligible eigenmode magnitudes.) It is well known that the right and left singular vectors can be used as the pre-processing and post-processing vectors such that the receiver can easily extract the data symbol without interference.

Define the eigenchannel coefficient A_{rmk} by $A_{rmk} = 1$ if user k is to use the mth subcarrier's rth eigenchannel and $A_{rmk} = 0$, otherwise. Then the received signal corresponds to subcarrier m of user k can be expressed as

$$\mathbf{y}_{mk} = \mathbf{H}_{mk} \sum_{i=1}^{R} \sum_{j=1}^{K} A_{imj}\sqrt{p_{imj}}\mathbf{t}_{imj}x_{imj} + \mathbf{n}_{mk}, \tag{4.2}$$

where x_{imj} denotes the data symbol of user j carried by the ith eigenchannel of subcarrier m. $\mathbf{T}_{imj}$ and p_{imj} are the pre-processing vector and transmit power, respectively. The entries of the $R_x \times 1$ noise vector $\mathbf{n}_{mk}$ are i.i.d. zero-mean complex Gaussian random variables with variance σ^2. x_{rmk}, the kth user's data symbol transmitted over the rth eigenchannel of subcarrier m, is pre-multiplied by the pre-processing vector $\mathbf{T}_{rmk}$ to form the T_x data symbols which are then transmitted with power p_{rmk}. Pre-multiplying the received signal $\mathbf{y}_{mk}$ by the post-processing vector $\mathbf{W}_{rmk}$, we obtain

$$\begin{aligned}\mathbf{r}_{rmk} &= \mathbf{w}^{\dagger}_{rmk}\mathbf{y}_{mk} \\ &= \mathbf{w}^{\dagger}_{rmk}\mathbf{H}_{mk}\sum_{i=1}^{R}\sum_{j=1}^{k} A_{imj}\sqrt{p_{imj}}\mathbf{t}_{imj}x_{imj} + \mathbf{w}^{\dagger}_{rmk}\mathbf{n}_{mk}\end{aligned}$$

where † denotes conjugate transpose.

4.3 Spatial Channel Assignment and Related Signal Processing

4.3.1 Orthogonal signal processing scheme

We use a simple example to illustrate the basic idea of the proposed scheme. Assume $T_x = R_x = 2, K = 2$ and the subcarrier m channel matrices for the two users, $\mathbf{H}_{m1}$ and $\mathbf{H}_{m2}$, are of full rank and have the SVDs

$$\begin{aligned}\mathbf{H}_{m1} &= \mathbf{U}_{m1}\mathbf{\Lambda}_{m1}\mathbf{V}^{\dagger}_{m1} \\ &= [\mathbf{u}^m_{11}\mathbf{u}^m_{12}]\begin{bmatrix} s^m_{11} & 0 \\ 0 & s^m_{12}\end{bmatrix}\begin{bmatrix}\mathbf{v}^{m\dagger}_{11} \\ \mathbf{v}^{m\dagger}_{12}\end{bmatrix}\end{aligned} \tag{4.3}$$

and

$$\begin{aligned}\mathbf{H}_{m2} &= \mathbf{U}_{m2}\mathbf{\Lambda}_{m2}\mathbf{V}^{\dagger}_{m2} \\ &= [\mathbf{u}^m_{21}\mathbf{u}^m_{22}]\begin{bmatrix} s^m_{21} & 0 \\ 0 & s^m_{22}\end{bmatrix}\begin{bmatrix}\mathbf{v}^{m\dagger}_{21} \\ \mathbf{v}^{m\dagger}_{22}\end{bmatrix}\end{aligned} \tag{4.4}$$

where $s^m_{11} = \max\{s^m_{ij} : i, j = 1, 2\}$. We assign the strongest eigenchannel to user 1 and allow user 2 to use one that is orthogonal to the strongest one. In other words, we use

$\mathbf{v}_{11}^m$ and $\mathbf{u}_{11}^m$ as the pre-processing vectors and assume those for user 2 are of the form $\bar{\mathbf{v}}_2^m = \alpha_1 \mathbf{v}_{21}^m + \alpha_2 \mathbf{v}_{22}^m$ and $\bar{\mathbf{u}}_2^m = \beta_1 \mathbf{u}_{21}^m + \beta_2 \mathbf{u}_{22}^m$, where α and β are weighting coefficients to be determined. The corresponding received signal from user 1 is given by

$$\mathbf{y}_{m1} = \mathbf{H}_{m1}(\sqrt{p_{m1}}\mathbf{v}_{11}^m x_{m1} + \sqrt{p_{m2}}\bar{\mathbf{v}}_2^m x_{m2}) + \mathbf{n}_{m1}, \tag{4.5}$$

which, after post-processing, becomes

$$\begin{aligned} \mathbf{r}_{1m1} &= \mathbf{u}_{11}^{m\dagger}\mathbf{y}_{m1} \\ &= \mathbf{u}_{11}^{m\dagger}\mathbf{H}_{m1}(\sqrt{p_{m1}}\mathbf{v}_{11}^m x_{m1} + \sqrt{p_{m2}}\bar{\mathbf{v}}_2^m x_{m2}) + \mathbf{n}_{m1} \\ &= \sqrt{p_{m1}} s_{11}^m x_{m1} + s_{11}^m(\alpha_1 \mathbf{v}_{11}^{m\dagger}\mathbf{v}_{21}^m + \alpha_2 \mathbf{v}_{11}^{m\dagger}\mathbf{v}_{22}^m)\mathbf{u}_{11}^m + \mathbf{u}_{11}^{m\dagger}\mathbf{n}_{m1}. \end{aligned} \tag{4.6}$$

To eliminate co-channel interference from user 2, we need

$$\alpha_1 = -\frac{\mathbf{v}_{11}^{m\dagger}\mathbf{v}_{22}^m}{\mathbf{v}_{11}^{m\dagger}\mathbf{v}_{21}^m}\alpha_2. \tag{4.7}$$

Similarly, to completely suppress interference into user 2's received waveform, we need

$$\beta_1 = -\frac{s_{22}^m \mathbf{v}_{22}^{m\dagger}\mathbf{v}_{11}^m}{s_{21}^m \mathbf{v}_{21}^{m\dagger}\mathbf{v}_{11}^m}\beta_2. \tag{4.8}$$

The resulting α's and β's should then be normalized such that the norm of the processing vectors are all equal to unity.

The received signal-to-noise ratio (SNR) for the two eigenchannels are given by

$$SNR_{m1(1)} = \frac{(s_{11}^m)^2 p_{m1}}{\sigma^2}, \tag{4.9}$$

$$SNR_{m2(2)} = \frac{(s_{21}^m \alpha_1 \beta_1 + s_{22}^m \alpha_2 \beta_2)^2 p_{m2}}{\sigma^2} \tag{4.10}$$

where the numbers in the subscript brackets denote the indices of the users who have the access to the corresponding eigenchannels.

To be more specific, if the BS wants to transmit the data to user k through the rth eigenchannel on subcarrier m, we should have

$$\mathbf{w}_{imj_i}^\dagger \mathbf{H}_{mj_i}\mathbf{t}_{rmk}\sqrt{p_{rmk}}x_{rmk} = 0 \qquad i = 1, \cdots, (r-1) \tag{4.11}$$

and

$$\mathbf{w}_{rmk}^{\dagger}\mathbf{H}_{mk}\mathbf{t}_{imj_i}\sqrt{p_{imj_i}}x_{imj_i} = 0 \qquad i = 1, \cdots, (r-1) \tag{4.12}$$

where j_i denotes the index of the user to whom the ith eigenchannel is assigned. Since $\mathbf{t}_{rmk}$ and $\mathbf{w}_{rmk}$ can be written as

$$\mathbf{t}_{rmk} = \sum_{l=1}^{r} \alpha_{kl}\mathbf{v}_{kl}^{m}, \tag{4.13}$$

$$\mathbf{w}_{rmk} = \sum_{l=1}^{r} \beta_{kl}\mathbf{u}_{kl}^{m} \tag{4.14}$$

(4.11) and (4.12) are equivalent to

$$\mathbf{w}_{imj_i}^{\dagger}\mathbf{H}_{mj_i}\left(\sum_{l=1}^{r} \alpha_{lk}\mathbf{v}_{kl}^{m}\right)\sqrt{p_{rmk}}x_{rmk} = 0 \qquad i = 1, \cdots, (r-1) \tag{4.15}$$

and

$$\left(\sum_{l=1}^{r} \beta_{lk}\mathbf{u}_{kl}^{m}\right)^{\dagger}\mathbf{H}_{mk}\mathbf{t}_{imj_i}\sqrt{p_{imj_i}}x_{imj_i} = 0 \qquad i = 1, \cdots, (r-1). \tag{4.16}$$

The above equations and the condition that the the precoding vectors should be normalized to render unity norm imply that the corresponding gain to noise ratio (GNR) is given by

$$\begin{aligned} GNR_{m1(k)} &= \frac{|s_{k1}|^2}{\sigma^2} \\ GNR_{mr(k)} &= \frac{\left|\sum_{i=1}^{r} \alpha_i\beta_i s_{ki}\right|^2}{\sigma^2},\ r \neq 1 \end{aligned} \tag{4.17}$$

Similarly, if user k wants to transmit the data to the BS through the rth eigenchannel on subcarrier m, the following identities should be satisfied.

$$\left(\sum_{l=1}^{r} \beta_{l}\mathbf{u}_{kl}^{m}\right)^{\dagger}\mathbf{H}_{mk}\mathbf{t}_{imj_i}\sqrt{p_{rmk}}x_{rmk} = 0 \qquad i = 1, \cdots, (r-1) \tag{4.18}$$

and

$$\mathbf{w}_{imj_i}^{\dagger}\mathbf{H}_{mj_i}\left(\sum_{l=1}^{r} \alpha_{l}\mathbf{v}_{kl}^{m}\right)\sqrt{p_{imj_i}}x_{imj_i} = 0 \qquad i = 1, \cdots, (r-1). \tag{4.19}$$

Our design philosophy is to force the user whose candidate transmit channels have weaker eigenmodes to “fit” the user(s) with stronger eigenmodes by transmitting over an eigenchannel which lies within the dual space of the space spanned by all previously selected eigenchannels. Each new eigenchannel is obtained by using proper processing vectors which are linear combinations of known eigenvectors. The process is similar to a Gram-Schmidt orthonormalization process except that the process follows the descending eigen-magnitude order. Hence, a precoder based on the above design procedure is henceforth referred to as a Gram-Schmidt (GS) precoder. Once the assignment and the orthogonalizing weighting coefficients of the first r eigenchannels are determined, the corresponding GNR can be computed accordingly.

4.3.2 Non-orthogonal signal processing scheme

In the previous subsection, we consider MIMO systems that use a orthogonal precoding scheme so that system users can transmit through distinct eigenchannels on the same subcarrier without causing interference to each other. For such a scheme, however, the maximum eigenchannel number is bounded by the rank of the MIMO channel matrix (R) and thus the spectrum efficiency may be constrained. To increase the spectrum efficiency, we allow more than R users to transmit over the eigenchannels on the same subcarrier. In this situation, the co-channel interference among users is no longer avoidable. Therefore, the associated optimization problem becomes more complicated due to the constraints on the tolerable inter-channel interference (ICI).

Based on the GS precoder design, we provide $R-1$ orthogonal eigenchannels for users with no interference and additional Q ($R \sim R+Q-1$) eigenchannels with various tolerable interference levels. For the $R-1$ orthogonal eigenchannels, the way to choose the pre-processing and post-processing vectors is the same as that described in previous subsection. That is, for the user to whom the rth eigenchannel is given, the pre-processing and post-processing vectors are the linear combinations of first r left and right singular vectors, respectively. In order that the Q non-orthogonal eigenchannels do not induce interference to the $R-1$ orthogonal eigenchannels, we require that the users who are allocated non-orthogonal eigenchannels to transmit over an eigenchannel which lies in the null space spanned by all $R-1$ orthogonal eigenchannels. More specifically, they use linear combinations of R singular vectors as the processing vectors to project the transmitting signal to the null space of the $R-1$ dimensional space spanned by orthogonal eigenchannels.

Although the non-orthoganal eigenchannels will not interfere with the $R-1$ orthogonal eigenchannels, the co-channel interference among the non-orthogonal eigenchannels is unavoidable. Here we define $B_{mk} = 1$ if user k is to transmit on the mth subcarrier's non-orthogonal eigenchannel and $B_{mk} = 0$, otherwise. The GINR (gain to interference and noise ratio) for users k who is allowed to transmit data on the non-orthogonal eigen-channels can be expressed as:

$$GINR_{mk} = \frac{\left(\sum\limits_{i=1}^{R} \alpha_{ki}\beta_{ki}s_{ki}\right)^2}{\sigma^2 + \sum\limits_{i=1, i\neq k}^{K} \left|\mathbf{w}_{mk}^{\dagger}\mathbf{H}_{mk}\mathbf{B}_{mi}\mathbf{t}_{mi}\right|^2 p'_{mi}} \tag{4.20}$$

If we define $\sum\limits_{i=1}^{R} \alpha_{ki}\beta_{ki}s_{ki}$ as g_{mk} (the channel gain of user k) and $\mathbf{w}_{mk}^{\dagger}\mathbf{H}_{mk}\mathbf{B}_{mi}\mathbf{t}_{mi}$ (the correlation between user k and user i) as ρ_{mki}, then (4.20) can be simplified as:

$$GINR_{mk} = \frac{|g_{mk}|^2}{\sigma^2 + \sum\limits_{i=1, i\neq k}^{K} |\rho_{mki}|^2 p'_{mi}} \tag{4.21}$$

It is noted that if a user is assigned more than one non-orthogonal eigen-channels, the interference will become too large since the correlation is unity. Therefore, we will assign one non-orthogonal eigenchannel to the same user at most.

4.4 Problem Formulation

Now we are ready to recast in mathematical form the RA problem of assigning subcarriers, and the corresponding power and the number of bits loaded to users such that the total transmit power of the system is minimized while the QoS of each user is satisfied.

Let R_k be the rate requirement for user k (bits/per OFDM symbol) and b_{rmk} the number of bits transmitted over the mth subcarrier using the rth eigenchannel. b_{max} denotes the maximum bit number (the highest modulation order) allowed to be carried by an eigenchannel. Moreover, let b'_{mk} and p'_{mk} be the number of bits and the corresponding power transmitted over the mth subcarrier using the non-orthogonal eigenchannel by user k. The RA problem can then be stated as

$$\min_{A_{rmk},p_{rmk},B_{mk},p'_{mk}} \sum_{m=1}^{M}\sum_{r=1}^{R-1}\sum_{k=1}^{K} A_{rmk}p_{rmk} + \sum_{m=1}^{M}\sum_{k=1}^{K} B_{mk}p'_{mk} \tag{4.22}$$

subject to the following constraints:

$$\sum_{r=1}^{R-1}\sum_{m=1}^{M} b_{rmk} + \sum_{m=1}^{M} b'_{mk} = R_k \qquad \forall \;\; k \tag{4.23}$$

$$\sum_{r=1}^{R-1}\sum_{k=1}^{K} A_{rmk} = R-1 \qquad \forall \;\; m \tag{4.24}$$

$$\sum_{k=1}^{K} B_{mk} = Q \qquad \forall \;\; m \tag{4.25}$$

$$A_{rmk} \in \{0,1\} \qquad \forall \; r,m,k \tag{4.26}$$

$$B_{mk} \in \{0,1\} \qquad \forall \; m,k \tag{4.27}$$

$$p_{rmk}, p'_{mk} \geq 0 \qquad \forall \;\; r,m,k \tag{4.28}$$

$$b_{max} \geq b_{rmk}, b'_{mk} \geq 0 \qquad \forall \;\; r,m,k \tag{4.29}$$

where $p_{rmk} = f(BER_k, b_{rmk}, GNR_{mr(k)})$ if $A_{rmk} = 1$ and $p_{rmk} = 0$, otherwise. BER_k represents user k's target BER and $f(\cdot,\cdot,\cdot)$ usually has a closed-form expression. If an M-ary quadrature amplitude modulation (M-QAM) is employed, then $f(\cdot,\cdot,\cdot)$ or p_{rmk} is given by [35]

$$p_{rmk} = \frac{1}{GNR_{mr(k)}} \ln\left(\frac{1}{5BER_k}\right) \frac{2^{b_{rmk}}-1}{1.5} \tag{4.30}$$

Moreover, the optimization problem becomes the orthogonal scheme via modifying (4.22), (4.24), (4.29) and omitting (4.23), (4.25), (4.27). Consequently, (4.22), (4.24), and (4.29) are modified as

$$\min_{A_{rmk}, p_{rmk}} \sum_{m=1}^{M} \sum_{r=1}^{R} \sum_{k=1}^{K} A_{rmk} p_{rmk}$$
$$\sum_{r=1}^{R} \sum_{k=1}^{K} A_{rmk} = R \; \forall \;\; m$$
$$b_{max} \geq b_{rmk} \geq 0 \; \forall \;\; r, m, k$$

Note that we only consider the case that $\sum_{i=1}^{K} R_i \leq RMb_{bmax}$ since if we have $\sum_{i=1}^{K} R_i > RMb_{bmax}$, the optimization problem will have no feasible solution. The above optimization problem is a mixed-integer problem which is NP-hard.

To find the optimal solution all transmission resources–subcarriers, eigenchannels, bits and power–should be jointly allocated, which, unfortunately requires very high computational complexity. Suboptimal solutions with modest complexity are perhaps more practical and desirable.

4.5 A ICI-Constrained Resource Allocation Algorithm

In this section, we propose a dynamic resource allocation algorithm for the non-orthogonal pre-coding scheme described above. The algorithm contains three steps. We assign the orthogonal eigenchannels and non-orthogonal eigenchannels in step one and step two, respectively. In the last step, we describe how to modify the conventional bit-loading algorithm such that it can be suitable for this case.

4.5.1 Step 1: an Space/Frequency Allocation Algorithm

In step one, we determine how to assign $R-1$ orthogonal eigenchannels to the users. Since the way to choose the pre-processing and post-processing vectors and the computation of the GNR for $R-1$ orthogonal eigenchannels is the same as mentioned in the previous section, we will assign $R-1$ orthogonal eigenchannels based on the proposed efficient space/frequency resource allocation algorithm described below.

We first determine the required eigenchannel number for each user and assign the eigenchannels to the users using a modified version of the two-phase algorithm of [36]-[37]. Then we use the conventional bit-loading algorithm to allocate bits over each user's eigenchannel subset and compute the required transmit power.

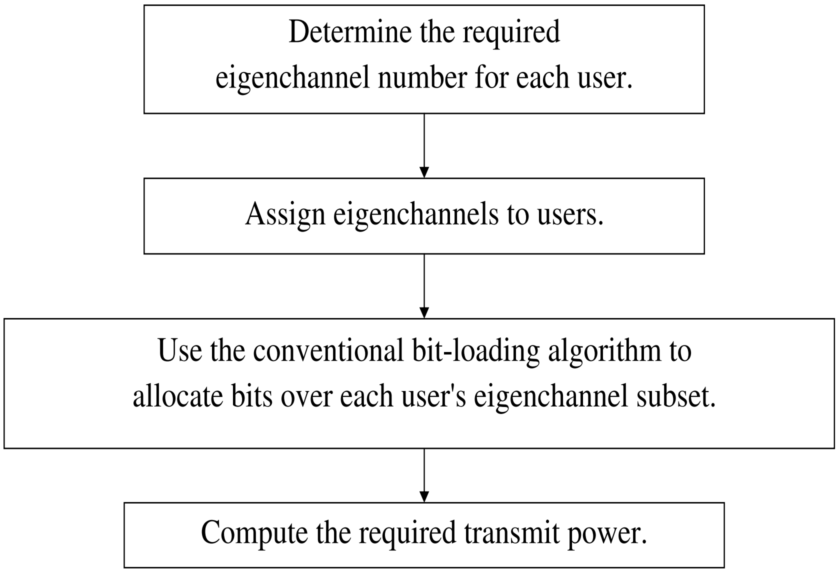

Figure 4.1: Flow Chart Description of Algorithm I.

In the first phase we compute the required eigenchannel number for each user according to the QoS and the *average channel condition.* For each subcarrier, say, the mth, we sort the maximum eigenmodes $\lambda_{max}(k,m)$ of the channel matrices $\mathbf{H}_{mk}, k = 1, 2, \cdots, K$ in descending order, i.e.,

$$\lambda_{max}(k_1, m) > \lambda_{max}(k_2, m) > \cdots > \lambda_{max}(k_K, m),$$

where

$$k_i = \arg \max_{k \in I_K \setminus \{k_1, k_2, k_{i-1}\}} \lambda_{max}(k,m), \text{ and } I_K = \{1, 2, \cdots, K\}$$

and set $A_{rmk} = 1$ if $k = k_r$. If $R < K$ we set $A_{Rmk} = 1$ for those $k = k_i, i > R$. The computing of the weighting coefficients and the corresponding GNR follow that

Table 4.1: Algorithm for computing the required eigenchannel number.

Step 1:	(assume T_k has been computed for all k according to (3.1)) (initialization) $c_k^{max} = \lceil R_k/b_{min} \rceil$; $c_k = c_k^{min} = \lceil R_k/b_{max} \rceil$ for each k

Step 2:	**while** $\sum_{k=1}^{K} c_k < RM$ **and** $c_k < c_k^{max}\ \forall k$
	  for $k = 1 : K$
	    if $c_k < c_k^{max}$
	     $\bar{P}_k = c_k \cdot f(BER_k, \frac{R_k}{c_k}, T_k)$
	     $\bar{P}_k^{new} = (c_k+1) \cdot f(BER_k, \frac{R_k}{(c_k+1)}, T_k)$
	     $\Delta P_k = \bar{P}_k - \bar{P}_k^{new}$
	    end
	  end
	  $w = \arg\max_k \Delta P_k$
	  $c_w = c_w + 1$
	end

described in Section II-B. Define the *average channel condition* for user k by

$$T_k = \frac{1}{M} \sum_{i=1}^{M} \sum_{j=1}^{R} A_{jik} GNR_{ij(k)}. \tag{4.31}$$

The minimum required eigenchannel number for user k is $\lceil R_k/b_{max} \rceil$. The actual eigenchannel number c_k is determined by iteratively verifying the relative reduction of the total transmit power after the allocation of an additional subcarrier. The detailed algorithm is given in Table. 4.1.

After determining c_k's, we then assign the eigenchannels on all subcarriers to each user based on the eigenmode magnitudes of the channel matrix and GNRs as described in the previous section. Let the kth eigenchannel of the mth subcarrier be represented by the two-tuple (k, m). The channel assignment follows the order $(1,1) \rightarrow (1,2) \rightarrow \cdots \rightarrow (1,M) \rightarrow (2,1) \rightarrow (2,2) \rightarrow \cdots \rightarrow (2,M) \rightarrow (3,1) \rightarrow \cdots$. That is, we assign the first eigenchannel on all subcarriers first, and then assign the second eigenchannel on all subcarriers, and so on. The ordering of subcarriers in the channel assignment process is important as once the eigenchannels of a subcarrier are assigned, no re-assignment is allowed. When assign rth eigenchannel on all subcarriers, we first sort the user on each subcarrier according to their $GNR_{mr(k)}$ in descending order and denote the largest $GNR_{mr(k)}$ on the mth subcarrier as Q_m and then sort subcarriers according to Q_m in descending order. Once the order of the subcarrier is determined, we assign the eigenchannel to the user with largest GNR; see Table 4.2 for details. After finishing channel assignment, we use the conventional bit-loading algorithm to allocate bits and compute the corresponding required transmit power for each user. This algorithm initially allocates zero bit to all subcarriers and then allocates bit by bit to the subcarrier which requires the least additional transmit power. The allocation process repeats until all data rate requirements are satisfied. The details of the bit-loading algorithm is given in Table 4.3. For a given set of assigned eigenchannels, the proposed bit-loading algorithm is optimal which we summarize below.

Lemma 4.5.1. *For a fixed eigenchannel assignment, the bit allocation algorithm described by Table 4.3 is optimal, i.e., it results in minimum power consumption.*

***Proof*.** For the given BER and the GNR of the eigenchannel assigned to user k, define $\Delta f(b_{rmk})$ as

$$\Delta f(b_{rmk}) = \begin{cases} f(BER_k, b_{rmk}, GNR_{mr(k)}) - f(BER_k, b_{rmk}-1, GNR_{mr(k)}), & \text{if } b_{rmk} \geq 1 \\ f(BER_k, b_{rmk}, GNR_{mr(k)}) - f(BER_k, 0, GNR_{mr(k)}), & \text{if } b_{rmk} < 1 \end{cases}$$

The author of [38] introduce necessary and sufficient conditions for a discrete bit allocation to be optimal:

1. $\Delta f(b_{rmk}) \leq \Delta f(b_{r'm'k}+1) \quad \forall r, r' = 1, 2, \ldots, R \text{ , } \forall m, m' = 1, 2, \ldots, M$ (efficient)
2. $\sum_{r=1}^{R} \sum_{m=1}^{M} b_{rmk} = R_k$ (B-tight)

Any bit distribution that satisfies the above conditions is an optimal solution. The second condition is clearly satisfied since the bit-loading algorithm will not stop until the loaded bits achieve the user data rate requirement. As for the first condition, we first show that $\Delta f(b_{rmk}+1) > \Delta f(b_{rmk})$ for all r, m and k. Since we use a closed form expression to estimate the require power when QAM modulation is used (4.30), we have

$$\begin{aligned}
\Delta f(b_{rmk}+1) &= f(BER_k, b_{rmk}+1, GNR_{mr(k)}) - f(BER_k, b_{rmk}, GNR_{mr(k)}) \\
&= \frac{1}{GNR_{mr(k)}} \ln\left(\frac{1}{5BER_k}\right) \frac{2^{b_{rmk}+1} - 2^{b_{rmk}}}{1.5} \\
&= \frac{1}{GNR_{mr(k)}} \ln\left(\frac{1}{5BER_k}\right) \frac{2^{b_{rmk}}}{1.5} \\
&> \frac{1}{GNR_{mr(k)}} \ln\left(\frac{1}{5BER_k}\right) \frac{2^{b_{rmk}-1}}{1.5} \\
&= \frac{1}{GNR_{mr(k)}} \ln\left(\frac{1}{5BER_k}\right) \frac{2^{b_{rmk}} - 2^{b_{rmk}-1}}{1.5} \\
&= \Delta f(b_{rmk}) \qquad \text{for } b_{rmk} > 0
\end{aligned}$$

and

$$\begin{aligned}
\Delta f(b_{rmk}+1) &= f\left(BER_k, b_{rmk}+1, GNR_{mr(k)}) - f(BER_k, b_{rmk}, GNR_{mr(k)}\right) \\
&= \frac{1}{GNR_{mr(k)}} \ln\left(\frac{1}{5BER_k}\right) \frac{2^{b_{rmk}+1} - 2^{b_{rmk}}}{1.5} \\
&= \frac{1}{GNR_{mr(k)}} \ln\left(\frac{1}{5BER_k}\right) \frac{2^{b_{rmk}}}{1.5} \\
&> 0 \\
&= \frac{1}{GNR_{mr(k)}} \ln\left(\frac{1}{5BER_k}\right) \frac{2^{b_{rmk}} - 0}{1.5} \\
&= \Delta f(b_{rmk}) \qquad \text{for } b_{rmk} = 0
\end{aligned}$$

If there exist a b_{rmk} and a $b_{r'm'k}$ in the result of the bit-loading algorithm such that $\Delta f(b_{rmk}) > \Delta f(b_{r'm'k}+1)$, this will contradict the step 2 in bit-loading process because when deciding to increase the bits of the rth eigenchannel on the mth subcarrier from $b_{rmk}-1$ to b_{rmk}, the power increment of loading a bit to the r'th eigenchannel on the m'th subcarrier is less than the power increment of loading a bit to the rth eigenchannel on the mth subcarrier. Therefore, the result of the bit-loading process must satisfy the first condition. □

One of the advantages of this algorithm is its low computational complexity. We need only to perform bit-loading for each user once; the complexity analysis is discussed

Table 4.2: The eigenchannel assignment algorithm.

Step 1: (initialization) Set all $A_{rmk} = 0$.
Step 2: **while** $c_k > 0\ \forall k$
  for $r = 1 : R$
    $Q_m = \max_k GNR_{mr(k)}$
    Arrange all subcarriers by decreasing order of Q_m such that $Q_1 \geq Q_2 \geq ... \geq Q_M$.
    for $m = 1 : M$
      Compute $GNR_{mr(k)} \forall k$ according to the previous 1∼(r-1) channel assignment process. Let $D_m = \{GNR_{mr(1)}, GNR_{mr(2)} ..., GNR_{mr(K)}\}$. (If $r = 1$, then let $GNR_{mr(k)} = \lambda_{max}(k, m)\ \forall k.$)
      while $\sum_{k=1}^{K} A_{rmk} = 0$
        $w = \arg\max_k GNR_{mr(k)} \in D_m$
        if $c_w > 0$
          $A_{rmw} = 1$, $c_w = c_w - 1$
        else
          $D_m = D_m - \{GNR_{mr(w)}\}$
        end
      end
    end
  end
end

later. Another advantage of this algorithm is that it considers not only the fairness but also the efficiency of the resource utilization. In step 1, we insure that every user is assigned enough eigenchannels to transmit data so that outage will not occur. In step 2, we assign eigenchannels to the user who has the highest eigenmode magnitude, making the most of the available spatial resources.

4.5.2 Step 2 and 3: Assignment of non-orthogonal eigenchannels and modified bit-loading algorithm

In Step two, since a user is given at most a non-orthogonal eigenchannel, there will be $\frac{K!}{(K\text{-}Q)!}$ possible choices. A natural choice is the one with the largest sum GINR.

Table 4.3: The conventional bit-loading algorithm.

Step 1: (initialization) Set all $b_{rmk} = 0$ and $p_{rmk} = 0$ for all r, m, k.

Step 2: **for** $k = 1 : K$

  while $\sum_{m=1}^{M} \sum_{r=1}^{R} A_{rmk} b_{rmk} < R_k$

    set $p_{min} = \infty$, $m_{index} = 0$, and $r_{index} = 0$

    for $m = 1 : M$

      for $r = 1 : R$

        if $A_{rmk} = 1$

          $p_{temp} = f(BER_k, b_{rmk} + 1, GNR_{mr(k)}) - f(BER_k, b_{rmk} + 1, GNR_{mr(k)})$

          if $p_{temp} < p_{min}$

            $m_{index} = m$,$r_{index} = r$,$p_{min} = p_{temp}$

          end

        end

      end

    end

    $b_{r_{index} m_{index} k} = b_{r_{index} m_{index} k} + 1$

    $p_{r_{index} m_{index} k} = p_{r_{index} m_{index} k} + p_{min}$

  end

end

Once all eigenchannels are allocated, we start to load the bits to the eigenchannels for each user. The conventional bit-loading procedure is not suitable for each user cannot be independently loaded due to the co-channel interference among the non-orthogonal eigenchannels. Similar scenario occurs in digital subscriber line (DSL) systems. [40] proposes a multi-user discrete bit-loading process for DSL systems. Our bit-loading algorithm thus consists of a mixture of the conventional bit-loading algorithm and the method proposed in [40]. The first part is to check the power increment after loading a bit to the orthogonal eigenchannels. This part is just the same as the conventional bit-loading algorithm since there is no interference between the orthogonal eigenchannels. The second part is to check the power increment after loading a bit to the non-orthogonal eigenchannels. Let $\mathbf{b}_m = [b'_{m1} \ b'_{m2} \ \cdots \ b'_{mK}]^T$. By [35], the required SINR for user j to transmit b'_{mj} through the orthogonal eigenchannel on subcarrier m can be expressed as:

$$\gamma_j(BER_j, b'_{mj}) = \ln\left(\frac{1}{5BER_j}\right)\frac{2^{b'_{mj}-1}}{1.5}. \tag{4.32}$$

The corresponding transmitting power p'_{mj} should satisfy

$$\frac{|g_{mj}|^2 p'_{mj}}{\sigma^2 + \sum\limits_{i=1,i\neq j}^{K} |\rho_{mki}|^2 p'_{mi}} \geq \gamma_j(BER_j, b'_{mj}) \quad \forall \;\; j, m \tag{4.33}$$

which can be rearranged in a matrix form:

$$(\mathbf{I} - \mathbf{C}_m)\mathbf{p}_m \succeq \mathbf{y}_m \quad \forall \;\; m \tag{4.34}$$

where

$$\{\mathbf{C}_m\}_{i,j} = \begin{cases} \dfrac{\gamma_j(BER_j, b'_{mj})|\rho_{mij}|^2}{|g_{mi}|^2}, & \text{for } i \neq j \\ 0, & \text{otherwise} \end{cases} \tag{4.35}$$

$$\mathbf{p}_m = [p'_{m1} \; p'_{m2} \; \cdots \; p'_{mK}]^T \tag{4.36}$$

$$\mathbf{y}_m = \left[\frac{\gamma_1(BER_1, b'_{m1})\sigma^2}{|g_{m1}|^2}, \frac{\gamma_2(BER_2, b'_{m2})\sigma^2}{|g_{m2}|^2}, \cdots, \frac{\gamma_K(BER_K, b'_{mK})\sigma^2}{|g_{mK}|^2}\right]^T. \tag{4.37}$$

Here $\mathbf{a} \succeq \mathbf{b}$ means the inequality holds element-wise. Then we can compute $\mathbf{p}_m$ by

$$\mathbf{p}_m = (\mathbf{I} - \mathbf{C}_m)^{-1}\mathbf{y}_m \quad \forall \;\; m. \tag{4.38}$$

If the solution $\mathbf{p}_m$ is all-positive then it is a feasible solution that satisfies (4.34). Otherwise, no feasible solution exists. The authors of [40] also show that if the solution of (4.34) exists and the elements of the solution vector are all positive, the Perron eigenvalue (that is, the largest positive eigenvalue) of $\mathbf{C}_m$, denoted as $\lambda(\mathbf{C}_m)$, must be less than 1. In addition, $\mathbf{p}_m$ computed by (4.38) is the Pareto optimal solution to (4.34). In other words, any positive vector that satisfies (4.34) is greater than or equal to $\mathbf{p}_m$ element-wise. The modified bit-loading algorithm is now described as follows:

1. Initialize $\mathbf{b}_m = [0\ 0\ \cdots\ 0]^T$ and $\mathbf{p}_m = [0\ 0\ \cdots\ 0]^T$ for $m = 1, 2, \cdots, M$.

2. Initialize $b_{rmk} = 0$ and $p_{rmk} = 0$ for all r, m, k.

3. For $k = 1, 2, \cdots, K$, if $\sum_{r=1}^{R} \sum_{m=1}^{M} b_{rmk} + \sum_{m=1}^{M} b'_{mk} < R_k$

   (a) check the smallest power increment after adding one bit among all orthogonal eigenchannels assigned to user k. Denote it as P_{1k} and record that it is belong to which orthogonal eigenchannel.

   (b) check the smallest power increment after adding one bit among all non-orthogonal eigenchannels assigned to user k by using (4.38). It is noted that we should confirm that the solution vector is positive by checking $\lambda(\mathbf{C}_m)$ is less than 1 or not. Denote it as P_{2k} and record that it is belong to which non-orthogonal eigenchannel.

   (c) Let $P(k)$ be the smaller one of P_{1k} and P_{2k} and record that the bit and the power increments are belong to which orthogonal (or non-orthogonal) eigenchannel.

4. Find the user k with the smallest $P(k)$ and add one bit to the corresponding orthogonal(or non-orthogonal) eigenchannel. Go back to step 3 if

$$\sum_{r=1}^{R} \sum_{m=1}^{M} b_{rmk} + \sum_{m=1}^{M} b'_{mk} < R_k, \ \forall\ k$$

.

4.6 Complexity Analysis and Simulation Results

4.6.1 Computational Complexity Analysis

In this subsection, we analyze the complexity of the proposed resource allocation algorithm for the non-orthogonal precoding scheme.

The assignment of the $R-1$ orthogonal eigenchannels is $O((R-1)M$ $+(R-1)\ (Klog_2K + Mlog_2M) + (R-1)M)$. For assigning the Q non-orthogonal eigenchannels, we check all $\frac{K!}{(K\text{-}Q)!}$ possible choices so the complexity is $O\left(M\frac{K!}{(K\text{-}Q)!}\right)$. Finally, the complexity of the bit-loading algorithm is $O\left(\sum_{k=1}^{K} R_k MR\right) = O(KR_{max}MR)$. Therefore, the total complexity is $O\left((R-1)M + (R-1)(Klog_2K + Mlog_2M) + (R-1)M + M\frac{K!}{(K\text{-}Q)!}\right.$ $\left.+KR_{max}MR\right) = O(KR_{max}MR)$.

4.6.2 Simulation Results

In this subsection, we evaluate the performance of the non-orthogonal precoding scheme and compare it with the performance of the orthogonal precoding scheme (using the space/frequency allocation algorithm).

The performance of the non-orthogonal precoding scheme and the orthogonal precoding scheme for downlink transmissions with different channel matrix rank value is shown in Fig. 4.2-4.4, respectively. The average power is normalized by that of the single-user case, i.e., when a single user has access to all eigenchannels and all subcarriers. We define the average power ratio at BER=B as :

$$\mathbf{P}_B = 10\log_{10}\left(\frac{P_{avg,B}}{P_{avg,10^{-5},single}}\right) \tag{4.39}$$

where $P_{avg,B}$ represents the average transmit power for a given modulation scheme at BER=B and $P_{avg,10^{-5},single}$ represents the average transmit power for the single user case at BER=10^{-5}.

We assume the number of the antenna at the BS and the MS are the same. The antenna number is from 3 to 5. Each entry of the channel matrix is i.i.d. zero-mean, unit-variance complex Gaussian The system has eight different modulation modes, BPSK, QPSK, 8QAM, 16QAM, 32QAM, 64QAM, 128QAM and 256 QAM, respectively. For simplicity, we assume that the required data rate and BER are the same for all users.

We can notice that when the rank of the channel matrix is 3, the performance of the non-orthogonal precoding scheme is about 1 dB worse than the orthogonal precoding scheme. However, when we increase the rank to 4 and 5, the performance of the non-orthogonal precoding scheme is better than the orthogonal precoding scheme by 0.7 and 1.8 dB, correspondingly.

The reason for this phenomenon is that for the rank 3 case, we provide 2 orthogonal eigenchannels and 2 non-orthogonal eigenchannels on each subcarrier in the non-orthogonal precoding scheme. However, in the orthogonal precoding scheme, we provide 3 orthogonal eigenchannels on each subcarrier in total. This means that for the non-orthogonal precoding scheme, we "sacrifice" 33% of the orthogonal eigenchannels to get Q non-orthogonal eigenchannels (in this case, Q=2). However, the gain of the non-orthogonal eigenchannels is not enough to compensate the loss of the orthogonal eigenchannels. For rank 4 and rank 5 cases, 25% and 20% of the orthogonal eigenchannels are sacrificed. This implies that when the rank of the MIMO channel matrix is increased, the impact of sacrificing the orthogonal eigenchannels is reduced. But for each case, we still provide Q non-orthogonal eigenchannels to users for the non-orthogonal pre-coding scheme. Therefore, when the rank of the MIMO channel matrix is increased, the advantage of the non-orthogonal pre-coding scheme will begin to appear.

In Fig. 4.5 and 4.6, the performance is not improved as we increase the value of Q. This contradicts the intuition that the larger Q provides more eigenchannels (with interference) than smaller Q. This is because the bit-loading algorithm used in the non-orthogonal precoding scheme is not guaranteed optimal. The optimality is destroyed by loading the bits to the non-orthogonal eigenchannel. Therefore, the result of the bit-loading algorithm used in the non-orthogonal precoding scheme may be the local optimal solution instead of global optimal solution. Thus, increasing the value of Q will not insure the better performance.

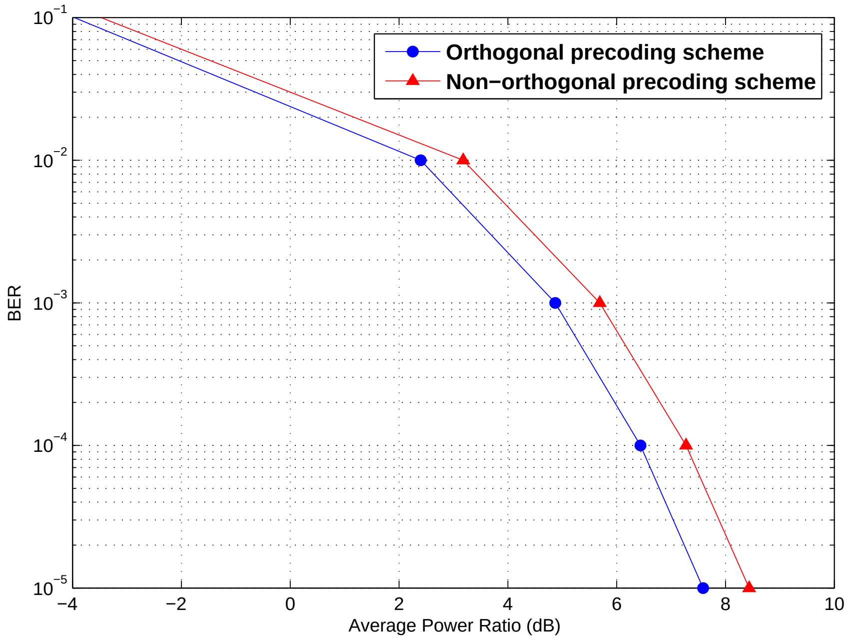

Figure 4.2: Average power ratio per user for a MIMO-OFDM downlink; 32 subcarriers, 128 bits per OFDM symbol, 4 users, rank=3.

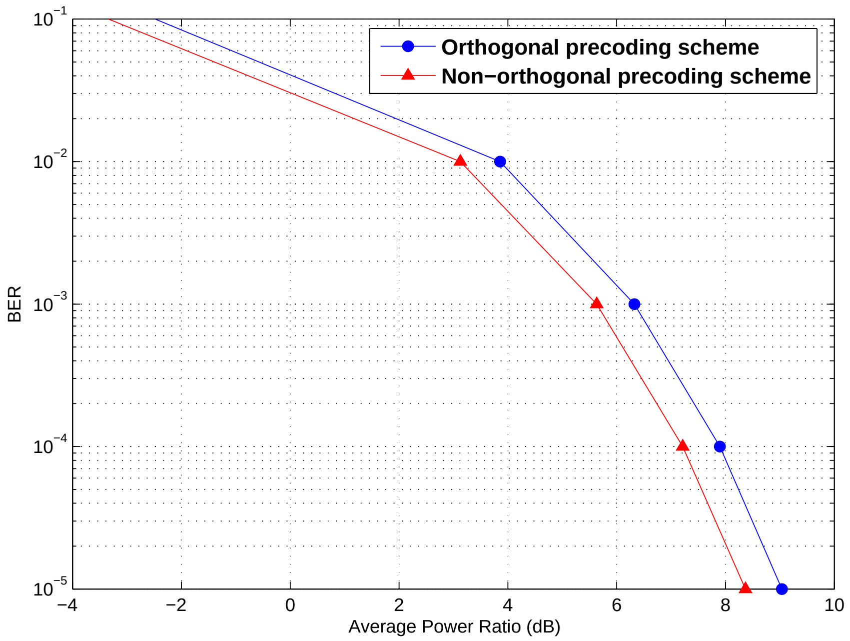

Figure 4.3: Average power ratio per user for a MIMO-OFDM downlink; 32 subcarriers, 192 bits per OFDM symbol, 4 users, rank=4.

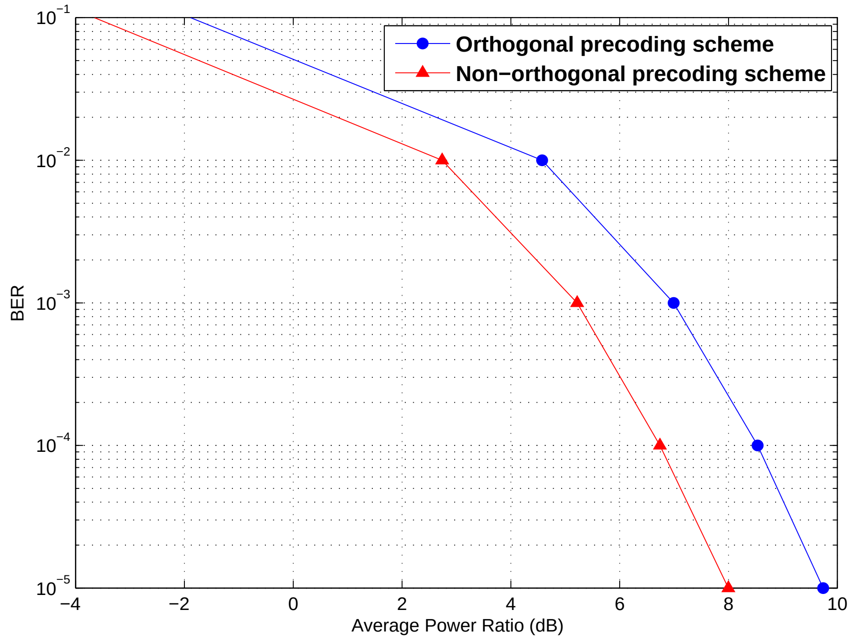

Figure 4.4: Average power ratio per user for a MIMO-OFDM downlink; 32 subcarriers, 240 bits per OFDM symbol, 4 users, rank=5.

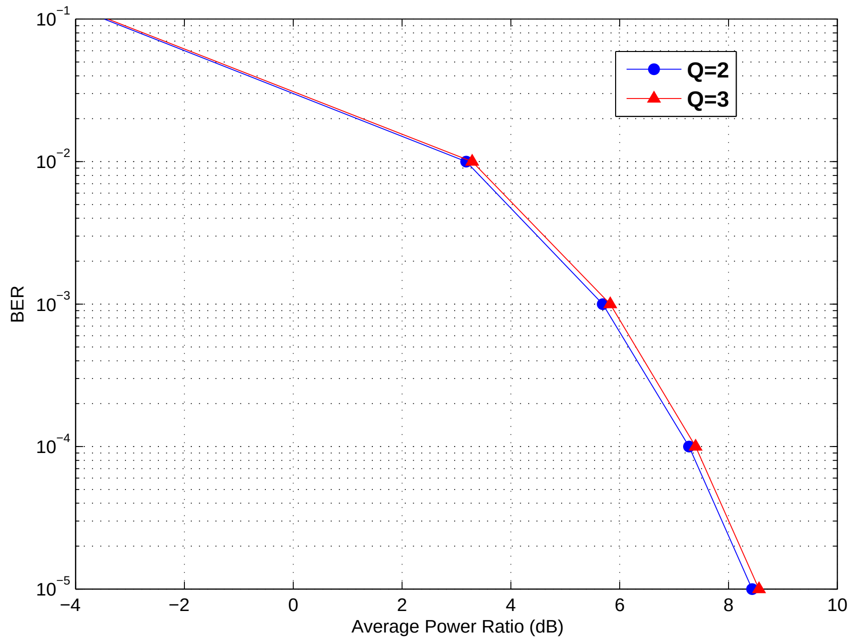

Figure 4.5: Average power ratio per user for a MIMO-OFDM downlink; 32 subcarriers, 144 bits per OFDM symbol, 4 users, rank=3.

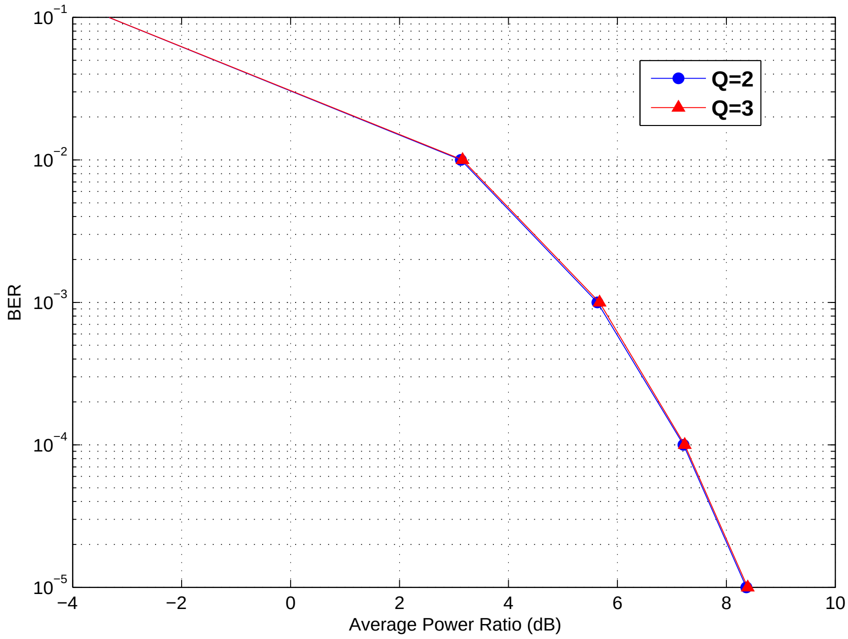

Figure 4.6: Average power ratio per user for a MIMO-OFDM downlink; 32 subcarriers, 192 bits per OFDM symbol, 4 users, rank=4.

Chapter 5

Resource Allocation for MIMO Systems with Codebook-based Precoding

The precoding schemes we considered so far require complete channel state information to achieve full performance gain. In a frequency-division duplex system, however, full channel state information must be conveyed through a feedback channel. This is not very efficient and practical due to the number of channel coefficients that needed to be quantized and sent back to the transmitter over limited bandwidth control channels.

Precoding schemes for spatial multiplexing systems with limited feedback capacity is more feasible in real-world applications [27]-[28]. The basic idea is that the transmit precoder is chosen from a finite set of precoding matrices, called the codebook, known to both the receiver and the transmitter. The receiver chooses the optimal precoder from the codebook as a function of the current channel state information and sends the binary index of this (precoder) matrix to the transmitter over a feedback channel. In this chapter, we discuss the resource optimization problem for codebook-based MIMO-OFDMA systems.

5.1 Transceiver Models and Precoding Criteria

5.1.1 System parameters and transceiver model

Again, we consider the uplink of a MIMO-OFDMA system with R_x transmit antennas at the base station and T_x receiver antennas at mobile stations. The frequency band is divided into M subcarriers. For the kth MS on the mth subcarrier, a bit stream is sent into a vector encoder and modulator block where it is demultiplexed into N different substreams. Each of the N bit substreams is then modulated independently using the same constellation $\mathcal{W}$. This yields a symbol vector of $\mathbf{s}_{mk} = [s_{mk}^1 \; s_{mk}^2 \; \ldots \; s_{mk}^N]^T$. For convenience, we will assume that $E[\mathbf{s}_{mk}^{\dagger}\mathbf{s}_{mk}] = \mathbf{I}_N$.

The symbol vector $\mathbf{s}_{mk}$ is then multiplied by an $T_x \times N$ precoding matrix $\mathbf{F}_{mk}$ producing a length T_x vector $\mathbf{x}_{mk} = \sqrt{\frac{E_m}{N}}\mathbf{F}_{mk}\mathbf{s}_{mk}$ where E_m is the total transmit energy on the subcarrier m, T_x is the number of transmit antennas, and $T_x > N$. We assume throughout the correspondence that $R_x > M$. Assuming perfect timing, synchronization, sampling, and a memoryless linear matrix channel, this formulation allows the baseband, discrete-time equivalent received signal to be written as

$$\mathbf{y}_{mk} = \sqrt{\frac{E_m}{N}}\mathbf{H}_{mk}\mathbf{F}_{mk}\mathbf{s}_{mk} + \mathbf{v}_{mk} \tag{5.1}$$

where $\mathbf{H}_{mk}$ is the channel matrix and $\mathbf{v}_{mk}$ is the noise vector. We assume that the the entries of $\mathbf{v}_{mk}$ are independent and distributed according to $\mathcal{CN}(0, N_o)$. The received vector is then decoded by a vector decoder, assuming perfect knowledge of $\mathbf{H}_{mk}\mathbf{F}_{mk}$, that produces a hard decoded symbol vector $\hat{\mathbf{s}_{mk}}$.

In this correspondence, the BS chooses a precoding matrix $\mathbf{F}_{mk}$ from a finite set of possible precoding matrices $\mathcal{F} = [\mathbf{F}_1 \; \mathbf{F}_2 \ldots \; \mathbf{F}_L]$ and conveys the index of the chosen precoding matrix back to the transmitter over a limited capacity , zero-delay feedback link.

At the receiver side, we consider linear receivers such as Zero-forcing (ZF) receiver and MMSE receiver instead of the ML receiver due to the lower complexity of linear receivers. Linear receivers apply an $N \times R_x$ matrix $\mathbf{G}_{mk}$, chosen according to some criterion, to produce $\hat{\mathbf{s}_{mk}} = Q(\mathbf{G}_{mk}\mathbf{y}_{mk})$ where $Q()$ is a function that performs single-dimensional ML decoding for each entry of a vector. For a ZF linear receiver, $\mathbf{G}_{mk} = (\mathbf{H}_{mk}\mathbf{F}_{mk})^{+}$. When a MMSE linear decoder is used, $\mathbf{G}_{mk} = [\mathbf{F}^{\dagger}_{mk}\mathbf{H}^{\dagger}_{mk}\mathbf{H}_{mk}\mathbf{F}_{mk} + (NN_o/E_m)\mathbf{I}_N]^{-1}\mathbf{F}^{\dagger}_{mk}\mathbf{H}^{\dagger}_{mk}$.

5.1.2 Precoding Criteria

In this subsection, we introduce the criteria for choosing the precoding matrix from the predetermined codebook $\mathcal{F}$. The author of [28] propose several precoding criteria for minimizing average BER or maximizing the system capacity. In this report, we focus on the criteria for minimizing average BER.

In [41], it is shown that in order to minimize a bound on the average probability of a symbol vector error, the minimum substream SNR must be maximized. It was also shown in [41] that the SNR of the nth substream on the mth subcarrier of the user k is given by

$$SNR^{(ZF)}_{mnk} = \frac{E_m}{NN_0[\mathbf{F}^{\dagger}_{mk}\mathbf{H}^{\dagger}_{mk}\mathbf{H}_{mk}\mathbf{F}_{mk}]^{-1}_{n,n}} \tag{5.2}$$

for the ZF receiver and

$$SNR^{(MMSE)}_{mnk} = \frac{E_m}{NN_0[\mathbf{F}^{\dagger}_{mk}\mathbf{H}^{\dagger}_{mk}\mathbf{H}_{mk}\mathbf{F}_{mk} + (NN_0/E_m)\mathbf{I}_N]^{-1}_{n,n}} - 1 \tag{5.3}$$

for the MMSE decoder, where $A_{n,n}$ is the entry (n, n) of A. Since the minimum substream SNR will dominate the BER performance, when we are choosing the precoding matrix F_{mk} from the codebook $\mathcal{F}$ for the user k on the $m$the subcarrier, we will choose the one with the maximum "minimum substream SNR." That is, we will choose the ith precoding matrix F_i such that

$$\mathbf{F}_{mk} = \arg\max_{\mathbf{F}_i \in \mathcal{F}} \min_{n=1\sim N} SNR_{mnk} \tag{5.4}$$

where SNR_{mnk} is determined by (5.2) or (5.3).

5.2 Problem Formulation

Instead of minimizing the total transmit power or maximizing the overall system capacity (throughput), we now choose to minimize the average BER performance with user peak power constraints and proportional subcarrier number fairness.

In order to avoid co-channel interference (CCI), we adopt the single-user-per-subcarrier policy, allowing each subcarrier to serve one user only. Define the subcarrier coefficient C_{mk} and let $C_{mk} = 1$ if user k is to transmit on the mth subcarrier and $C_{mk} = 0$, otherwise. Denote the transmit power of the nth substream on the mth subcarrier of user k as p_{mnk}. Then resource allocation problem is equivalent to solving the following optimization problem.

$$\arg \min_{C_{mk}, p_{mnk}} \frac{1}{MNK} \sum_{m=1}^{M} \sum_{n=1}^{N} \sum_{k=1}^{K} C_{mk} BER_{mnk} \tag{5.5}$$

subject to the constraints:

$$\sum_{m=1}^{M} C_{m1} : \sum_{m=1}^{M} C_{m2} : \ldots : \sum_{m=1}^{M} C_{mk} = R_1 : R_2 : \ldots : R_K \tag{5.6}$$

$$\sum_{k=1}^{K} C_{mk} = 1 \ \forall \ m \tag{5.7}$$

$$C_{mk} \in \{0, 1\} \ \forall \ m, k \tag{5.8}$$

$$p_{mnk} \geq 0 \ \forall \ r, m, k \tag{5.9}$$

$$\sum_{m=1}^{M} \sum_{n=1}^{N} C_{mk} p_{mnk} = \bar{P} \ \forall \ k \tag{5.10}$$

where R_k denotes the date rate of user k and $\bar{P}$ is the user's power constraint. The constraint (5.6) means that the subcaarier numbers assigned to users are proportional to the user's data rates. As mentioned before, if an M-ary quadrature amplitude modulation (M-QAM) is employed, then BER_{mnk} or p_{rmk} is given by [35]

$$BER_{mnk} = \frac{1}{5} \exp\left(-SNR_{mnk} \frac{1.5}{2^b - 1}\right) \tag{5.11}$$

where b is the number of transmit bits of each substream.

5.3 Resource Allocation Algorithms

In this section, we propose two adaptive resource allocation algorithms for both subcarrier assignment and power loading.

5.3.1 The Subcarrier Assignment Algorithm

As mentioned in the previous section, in order to minimize average user's BER, we have to maximize the minimum substream SNR. Thus we will assign subcarriers based on the minimum substream SNR of each user.

First, the subcarrier number of each user will be determined by the user's data rate such that

$$c_1 : c_2 : \ldots : c_K = R_1 : R_2 : \ldots : R_K \tag{5.12}$$

where c_k is the subcarrier number of the user k. After determining the subcarrier number of each user, we then begin to assign subcarriers to the user. We assumed that the total power of user k is equally distributed to the all substreams on the subcarriers assigned to the user k. Thus SNR of the nth substream on the mth subcarrier of the user k is given by

$$SNR_{mnk}^{(ZF)} = \frac{E_m}{NN_0[\mathbf{F}_{mk}^{\dagger}\mathbf{H}_{mk}^{\dagger}\mathbf{H}_{mk}\mathbf{F}_{mk}]_{n,n}^{-1}} \tag{5.13}$$

for the ZF receiver and

$$SNR_{mnk}^{(MMSE)} = \frac{E_m}{NN_0[\mathbf{F}_{mk}^{\dagger}\mathbf{H}_{mk}^{\dagger}\mathbf{H}_{mk}\mathbf{F}_{mk} + (NN_0/E_m)\mathbf{I}_N]_{n,n}^{-1}} - 1 \tag{5.14}$$

for the MMSE decoder, as described in the previous section. The ordering of subcarriers in the subcarrier assignment process is important as once the subcarriers are assigned, no re-assignment is allowed. We first sort the user on each subcarrier according to their minimum substream SNR in descending order and denote the largest SNR_{mnk} on the

mth subcarrier as Q_m and then sort subcarriers according to Q_m in descending order. Once the order of the subcarrier is determined, we assign the subcarrier to the user with largest minimum substream SNR. If that user has been assigned enough subcarriers, then the current subcarrier will assigned to the remained users with largest minimum substream SNR. The detail can be checked in Table 5.1.

Table 5.1: The subcarrier assignment algorithm.

Step 1:	(initialization) Set all $C_{mk} = 0$.
Step 2:	**for** $m = 1 : M$
	for $k = 1 : K$
	$d_{mk} = min_n SNR_{mnk}$
	end
	$Q_m = \max_k d_{mk}$
	end
	Arrange all subcarriers by decreasing order of Q_m such that $Q_1 \geq Q_2 \geq ... \geq Q_M$.
Step 3:	**while** $c_k > 0 \ \forall k$
	for $m = 1 : M$
	Let $D_m = \{d_{m1}, d_{m2}, d_{m3}, ..., d_{mK}\}$.
	while $\sum_{k=1}^{K} C_{mk} = 0$
	$w = \arg\max_k d_{mk} \in D_m$
	if $c_w > 0$
	$C_{mw} = 1$, $c_w = c_w - 1$
	else
	$D_m = D_m - \{d_{mw}\}$
	end
	end
	end
	end

5.3.2 The Power Loading Scheme

In the previous subsection, we assume that the total power of user k is equally distributed to the all substreams on the subcarriers assigned to the user k and perform dynamic subcarrier assignment to extract the diversity gain of multiuser MIMO-OFDMA systems.

In this subsection, we consider the dynamic power loading to further enhance the overall system performance.

As discussed before, our goal is to minimize the average BER. In [42], the author had derived how to obtain the optimum power allocation for minimizing BER in multicarrier systems. Now we follow the method proposed in [42] to get the optimal power loading for the codebook based MIMO-OFDMA systems.

Since the subcarrier assignment has been done in previous subsection and we allow at most one user to transmit signals on each subcarrier, there is no co-channel interference and therefore the multiuser power loading is then decoupled into single user case. That is, we can deal with the power allocation for each user individually.

The BER for the nth substream on the mth subcarrier is generally a function of the corresponding power and GNR (gain to noise ratio), like (5.11). Because (5.11) is a convex function with respect to the power p_{mnk}, we can use the Lagrange multiplier method with the total power constraint. The Lagrangian function of user k may be expressed as

$$J(P_{k_1 1k}, P_{k_1 2k}, \ldots, P_{k_{c_k} Nk}) = \frac{1}{c_k N} \sum_{t=1}^{c_k} \sum_{n=1}^{N} BER_{k_t nk} + \lambda_k (\sum_{t=1}^{c_k} \sum_{n=1}^{N} p_{k_t nk} - \bar{P}) \quad (5.15)$$

where $k_1 \sim k_{c_k}$ is the subcarrier index assigned to the user k and λ_k denotes the Lagrange multiplier. By differentiating (5.15) with respect to $p_{k_t nk}$ and setting it to zero, we obtain a set of equations as

$$\frac{1}{c_k N} \frac{\partial BER_{k_t nk}}{\partial p_{k_t nk}} + \lambda_k = 0 \qquad k = 1, 2, 3, \ldots, K. \quad (5.16)$$

As mentioned before, $BER_{k_t nk}$ is the function of $p_{k_t nk}$ and $GNR_{k_t nk}$ (5.11). After some computation, we can get

$$p_{k_t nk} = \frac{2^b - 1}{1.5 GNR_{k_t nk}} \ln \left(\frac{0.3 GNR_{k_t nk}}{c_k N \lambda_k (2^b - 1)} \right). \quad (5.17)$$

But (5.17) still depends on the Lagrange multiplier λ_k. So we take (5.17) into the user's power constraint $\sum_{t=1}^{c_k}\sum_{n=1}^{N} p_{k_t n k} = \bar{P}$ and then we can express λ_k as

$$\lambda_k = \exp\left(-\frac{\bar{P} - \sum_{t=1}^{c_k}\sum_{n=1}^{N} \frac{2^{b-1}}{1.5GNR_{k_t n k}} \ln(\frac{0.3GNR_{k_t n k}}{c_k N(2^b-1)})}{\sum_{t=1}^{c_k}\sum_{n=1}^{N} \frac{2^{b-1}}{1.5GNR_{k_t n k}}} \right). \tag{5.18}$$

Thus, the corresponding power can then be computed. It is noted that if some substreams' power is negative after the computation, it means that the GNRs of these substream are too low and these substreams should not be allocated any power in order not to deteriorate the overall performance. In such case, we should exclude these substreams and do the Lagrange multiplier method again until the power of all substreams are not negative.

5.4 Complexity Analysis and Numerical Results

5.4.1 Computational Complexity Analysis

In this subsection, we analyze the complexity of the subcarrier assignment algorithm and the power loading algorithm.

For the subcarrier assignment algorithm, the complexity of step 2 is $O(KNlog_2N + MKlog_2K + Mlog_2M)$, and for step 3 the complexity is $O(MK)$, so the total complexity of the subcarrier assignment algorithm is $O(KNlog_2N + MKlog_2K + Mlog_2M + MK) = O(MKlog_2K)$. And for the power loading algorithm, the complexity is $O(NM)$.

5.4.2 Numerical Results

Selected simulated performance of the proposed resource allocation algorithm are presented in this subsection. First the performance of the subcarrier assignment algorithm for the codebook based MIMO-OFDAM systems is shown in Fig. 5.1-5.4. For Fig. 5.5-5.7, we evaluate the performance of the proposed power-loading algorithm.

We assume each $\mathbf{H}_{mk}$ is a 4×2 (4 antennas at the BS and 2 antennas at each MS) matrix for 2 substream codebook and 4×3 (4 antennas at the BS and 3 antennas at each MS) matrix for 3 substream codebook with i.i.d. zero-mean, unit-variance complex Gaussian entries. The system's modulation mode is BPSK. For simplicity, we assume that the required data rate are the same for all users. The codebook used here is from 802.16e standard.

In Fig. 5.1 and 5.2, we compare the subcarrier assignment algorithm for the ZF receiver with fixed subcarrier assignment scheme. From the figures we can find that the performance of the dynamic subcarrier assignment is better than fixed subcarrier assignment by almost 4dB at BER=10^{-2} for the 2 substream case and more than 4dB at BER=10^{-2} for the 3 substream case. The same result can also be found when the MMSE receiver is used (Fig. 5.3 and 5.4). The performance of the dynamic subcarrier assignment is better than fixed subcarrier assignment by 3dB at BER=10^{-2} for the 2 substream case and 2.5 dB at BER=10^{-2} for the 3 substream case.

For the dynamic power loading algorithm, we compare the performance of it with the equally power distributed system. We consider three different scheme:fixed subcarrier assignment without codebook precoding, fixed subcarrier assignment with codebook precoding and dynamic subcarrier assignment with codebook precoding. Here we assume QPSK modulation is used. In Fig. 5.5, using the dynamic power loading algorithm will provide nearly 1.5dB gain at BER=10^{-2} over the equally power distributed system in the fixed subcarrier assignment without codebook precoding environment. In Fig. 5.6, the dynamic power loading algorithm also achieves approximately 1dB gain at BER=10^{-2} in the fixed subcarrier assignment with codebook precoding environment. Finally, in Fig. 5.7, the dynamic power loading algorithm is superior to the equally power distributed system in the dynamic subcarrier assignment with codebook precoding environment by more than 1.5dB at BER=10^{-4}.

These figures (Fig. 5.5-5.7) also show that the improvement of the dynamic power-loading algorithm is more obvious in the fixed subcarrier assignment without codebook precoding environment. This is because that without precoding, the variation of the channel condition is much larger. Simulation results show that the variance of GNR is reduced by almost 50% after precoding. Therefore, the performance gain offered by the power-loading algorithm is smaller in the other two cases.

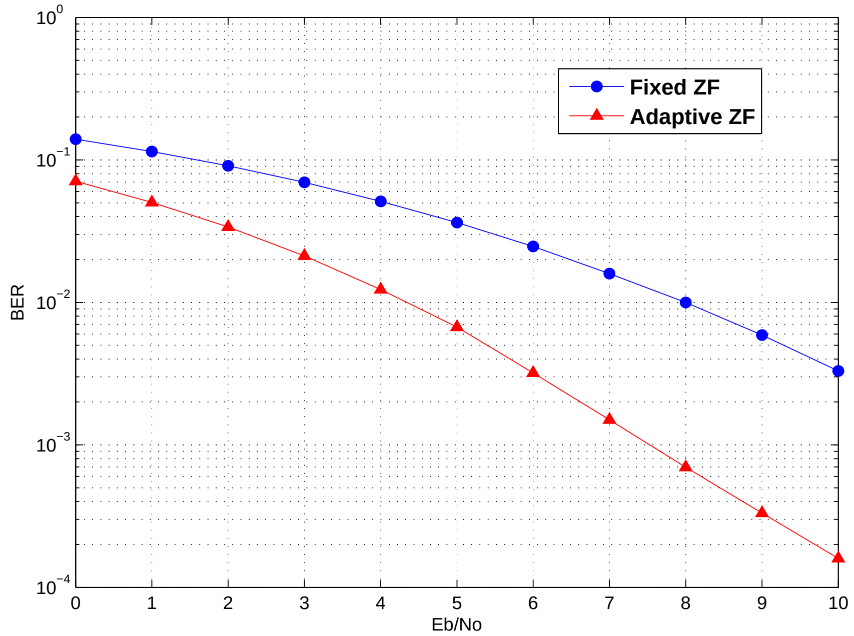

Figure 5.1: Average BER performance for the ZF receiver ; 128 subcarriers, 8 users, 2 substreams.

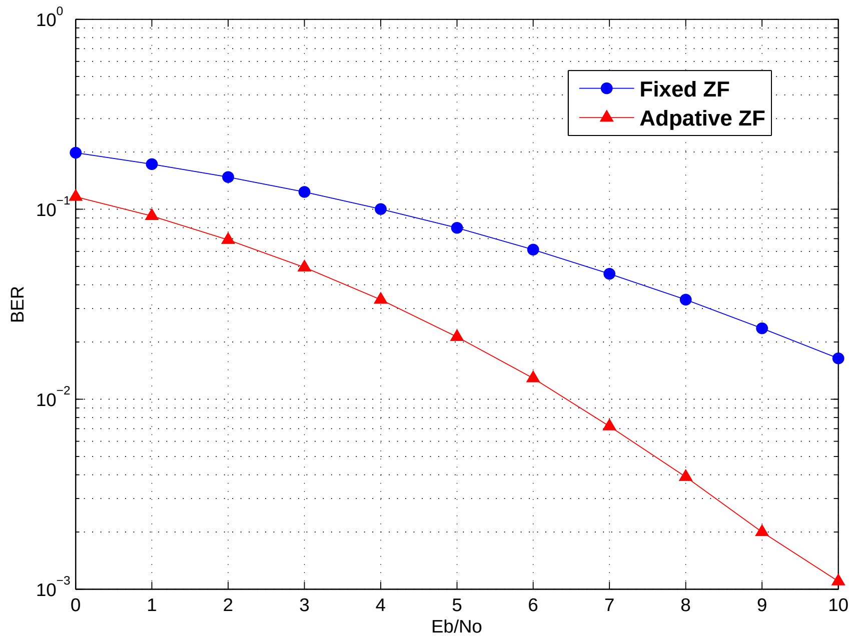

Figure 5.2: Average BER performance for the ZF receiver ; 128 subcarriers, 8 users, 3 substreams.

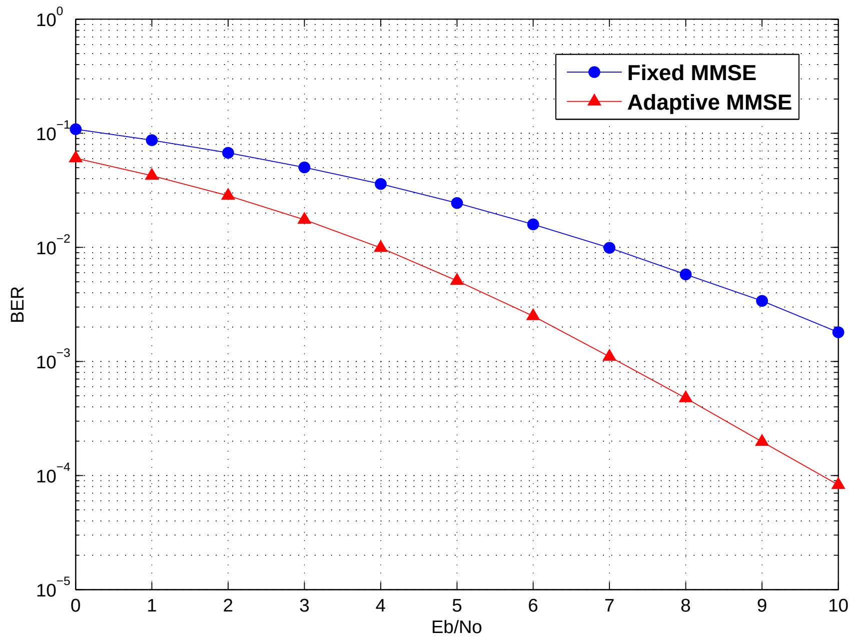

Figure 5.3: Average BER performance for the MMSE receiver ; 128 subcarriers, 8 users, 2 substreams.

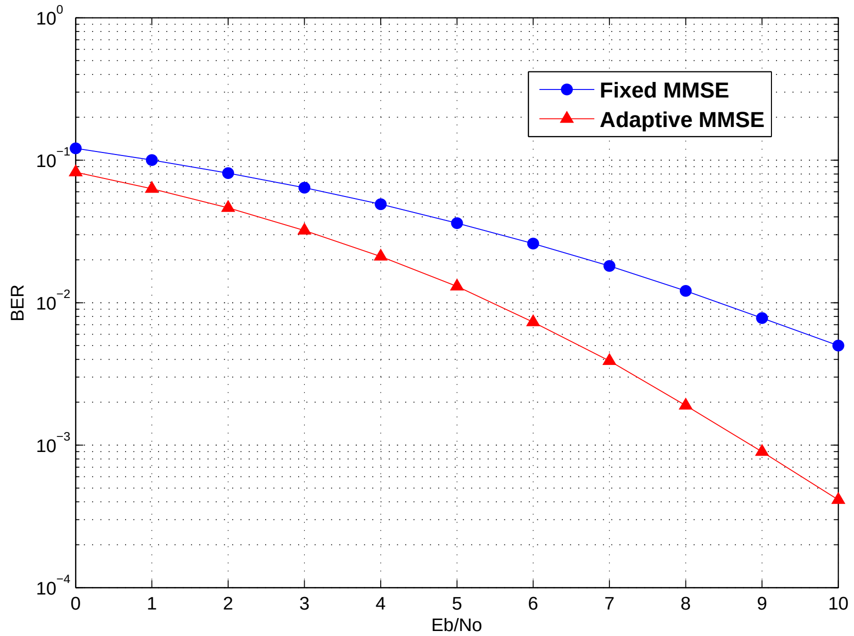

Figure 5.4: Average BER performance for the MMSE receiver ; 128 subcarriers, 8 users, 3 substreams.

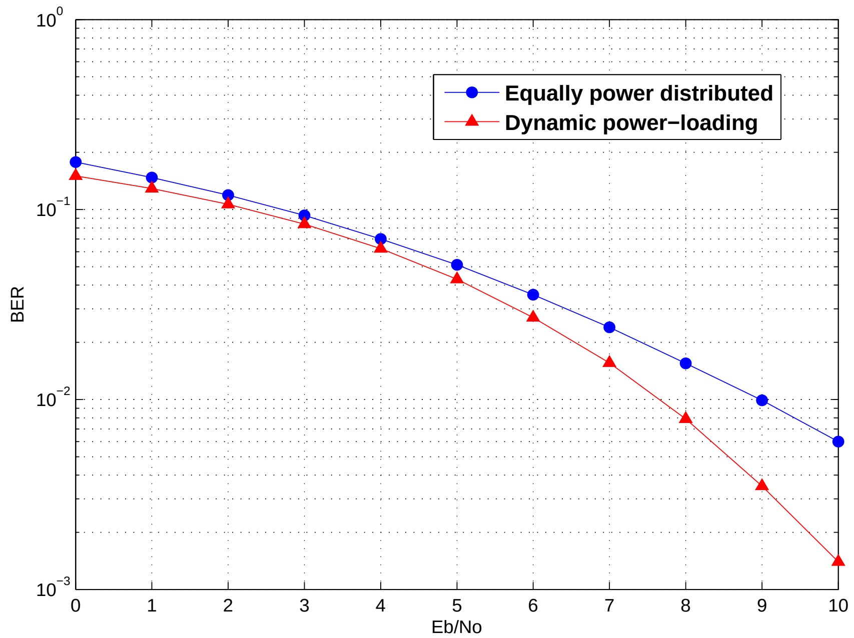

Figure 5.5: Average BER performance for the ZF receiver; fixed subcarrier assignment without codebook precoding ; 128 subcarriers, 16 users, 2 substreams.

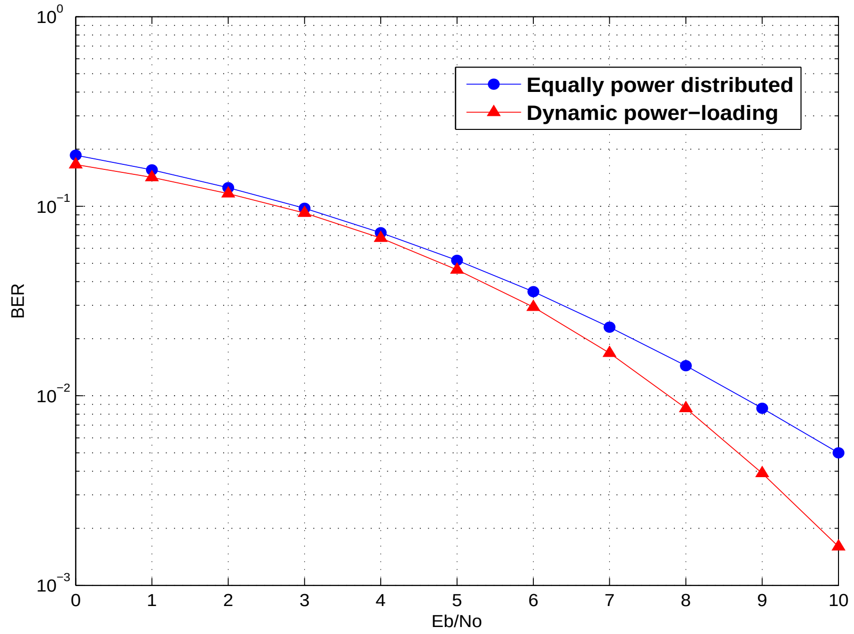

Figure 5.6: Average BER performance for the ZF receiver ; fixed subcarrier assignment with codebook precoding ; 128 subcarriers, 16 users, 2 substreams.

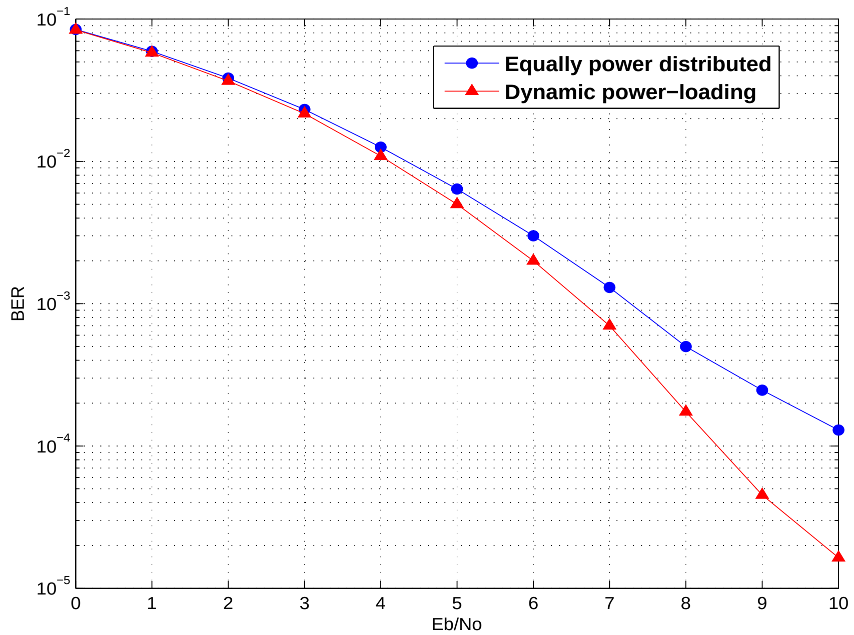

Figure 5.7: Average BER performance for the ZF receiver ; dynamic subcarrier assignment with codebook precoding ; 128 subcarriers, 16 users, 2 substreams.

Chapter 6

Conclusion

In this report, we first review the work of the first and second year and the detail can be found in the previous reports. In the final year, we consider the allocation of radio resources in a MIMO-OFDMA system. It is critical in maximizing resource efficiency, system capacity, and mitigating interference. We have presented two SVD-based precoding schemes (orthogonal and non-orthogonal precoding) that minimize the total consumed power while meeting various rate and SINR requirements. Since the orthogonal precoding scheme is applied only when the number of user is small or equal to the rank of channel, we extend our concern to non-orthogonal precoding schemes that guarantee zero or limited co-channel interference to further increase the spectrum efficiency. An adaptive resource allocation algorithm is proposed and its numerical performance is given. It is found that the lift of the orthogonal constraint leads to improved performance when the rank of the channel matrix is sufficient.

We also consider the resource allocation issue for spatial multiplexing systems with limited feedback (codebook based precoding) and present subcarrier assignment and power loading algorithms that minimize the average BER performance. The simulation results show that these dynamic resource allocation methods do indeed yield low average BER performance.

Some results in these three years have also been published in conferences and the associated information are listed below.

[43] J.-Y. Liu and Y.T. Su, "Performance Analysis of Transform Domain Communication Systems in the Presence of Spectral Mismatches" , in *Proc. Military Commun. Conf. (MILCOM),* Orlando, FL., USA, Oct. 28-31, 2007.

[44] Y.-S. Lu, Y.-B. Lin, and Y.T. Su, "Dynamic Resource Allocation for Relay-Based OFDMA Systems with Fairness Considerations," in *Proc. IEEE Wireless Commun. and Networking Conf. (WCNC)*, Sydney, NSW, Apr. 8-21, 2010.

[45] C.-L. Weng, Y.-B. Lin, and Y.T. Su, "Resource Allocation for MIMO-OFDMA Based Wireless Networks," in *Proc. IEEE Wireless Commun. and Networking Conf. (WCNC)*, Sydney, NSW, Apr. 8-21, 2010.

Bibliography

[1] V. Chakravarthy, A.K. Shaw, M.A. Temple, J.P. Stephens, "Cognitive radio - an adaptive waveform with spectral sharing capability," in *Proc. Wireless Commun. and Networking Conf.*, vol 2, 13-17 pp. 724-729. Mar. 2005.

[2] M. J. Lee et al., "Wavelet domain communication system: bit error sensitivity characterization for geographically separated transceivers ," in *Proc. Military Commun. Conf. (MILCOM)*, Anaheim, CA, vol. 2, pp. 1378-82. Oct. 2002.

[3] V. Chakravarthy, A.S. Nunez, J.P. Stephens, A.K. Shaw, M.A. Temple, "TDCS, OFDM, and MC-CDMA: A Brief Tutorial," *IEEE. Commun. Mag.*, vol 43, issue 9, pp. 11 - 16. Sep. 2005.

[4] M.K. Simon, M. Alouini, "A unified approach to the performance analysis of digital-communication over generalized fading channels," *IEEE. Proc.*, vol 86, issue 9, pp. 1860-1877. Sep. 1998.

[5] W. Rhee and J. M. Cioffi, "Increasing in Capacity of Multiuser OFDM system Using Dynamic Subchannel Allocation," in *Proc. IEEE Int. Veh. Tech. Conf.*, vol. 2, pp. 1085-1089, Spring 2000.

[6] L. Vandendorpe, R. T. Duran, J. Louveaux, and A.Zaidi, "Power Allocation for OFDM Transmission with DF Relaying," in *Proc. IEEE Int. Commun. Conf. (ICC),* May 2008, pp. 3795-3800.

[7] K. Seong, M. Mohseni, and J. M. Cioffi, “Optimal Resource Allocation for OFDMA Downlink Systems,” in *IEEE Int. Symp. Inform. Theory (ISIT),* pp.1394-1398, July 2006.

[8] T. C.-Y. Ng and W. Yu, “Joint optimization of relay strategies and resource allocations in a cooperative cellular network,” *IEEE J. Sel. Areas Commun.,* vol. 25, no. 2, pp. 328-339, Feb. 2007.

[9] M. Kaneko and P. Popovski, “Adaptive Resource Allocation in Cellular OFDMA System with Multiple Relay Stations,” in *IEEE Veh. Technol. Conf. (VTC-Springl),* pp. 3026-3030, April 2007.

[10] Z. Shen, J. G. Andrews, and B. L. Evans, “Adaptive resource allocation in multiuser OFDM systems with proportional rate constraints,” *IEEE Trans. Wireless Commun.,* vol. 4, pp. 2726-2737, November 2005.

[11] G. Li and H. Liu, “Resource Allocation for OFDMA Relay Networks With Fairness Constraints,” *IEEE J. Sel. Areas Commun.,* vol. 24, no. 11, pp. 2061-2069, Nov. 2006.

[12] R. U. Nabar, H. Bolcskei and F. W. Kneubuhler, “Fading Relay Channels: Performance Limits and Space-Time Signal Design,” *IEEE J. Sel. Areas Commun.,* vol. 22, no.6, pp. 1099-1109, August 2004.

[13] X. Qiu, K. Chawla, “On the Performance of Adaptive Modulation in Cellular Systems,” *IEEE Trans. Commun.,* 47 (6): pp.884-895, 1999.

[14] S. Sadr, A. Anpalagan, and K. Raahemifar, “A Novel Subcarrier Allocation Algorithm for Multiuser OFDM System With Fairness: User’s Perspective,” *IEEE Veh. Technol. Conf. (VTC),* pp. 1772-1776, Sep. 2007.

[15] S. Musa and W. Wasylkiwskyj, “Co-Channel Interference of Spread Spectrum Systems in a Multiple User Environment,” *IEEE Trans. Commun.,* pp.1405-1413, Oct. 1978.

[16] M. K. Awad and X. Shen, ”OFDMA Based Two-hop Cooperative Relay Network Resources Allocation,” in *Proc. IEEE Int. Commun. Conf. (ICC),* pp.4414-4418, Aug. 2008.

[17] X. Lu Z. li, J. Cai and X. Chen, “An Adaptive Resource Allocation Algorithm Based on Spatial Subchannel in Multiuser MIMO/OFDM Systems,” in *Proc. IEEE Int. Commun. Conf. (ICC),* pp. 4532-4536, MAY. 2008.

[18] H. Tian, S. Wang, Y. Gao, Q. Sun and P. Zhang, “A QoS-Guarantee Resource Allocation Scheme in Multi-user MIMO-OFDM Systems,” in *Proc. IEEE Veh. Technol. Conf. (VTC’07),* pp. 1802-1806, Sept. 2007.

[19] N. Leng, S. Yang, Y. Lu and L. Qi,“Dynamic Spatial Subcarrier and Power Allocation for Multiuser MIMO-OFDM System,” in *Proc. IEEE Int. Wireless Commun. Conf. (WiCOM’07),* pp. 180-183, Sept. 2007.

[20] M. S. Maw and S. I,“Resource Allocation Scheme in MIMO-OFDMA System for User’s Different Data Throughput Requirements,” in *Proc. IEEE Wireless Commun. and Networking Conf. (WCNC’07),* pp. 1706-1710, Mar. 2007.

[21] G. Liu, X. Liu and P. Zhang,“QoS oriented dynamical resource allocation for eigen beamforming MIMO OFDM,” in *Proc. IEEE Veh. Technol. Conf. (VTC’05),* vol.3 pp. 1450-1454, Sept. 2005.

[22] Y. Tan and Q. Chang,“Multi-user MIMO-OFDM with Adaptive Resource Allocation over Frequency Selective Fading Channel,” in *Proc. IEEE Int. Wireless Commun. Conf. (WiCOM’08),* pp. 1-5, Oct. 2008.

[23] P. Uthansakul and M.E. Bialkowski, "An Efficient Adaptive Power and Bit Allocation Algorithm for MIMO OFDM System Operating in a Multi User Environment," in *Proc. IEEE Veh. Technol. Conf. (VTC'06),* Vol.3 pp. 1531-1535, May. 2006.

[24] Z. Hu, G. Zhu, X. Xiao and Z. Chen, "Resource allocation for multiuser space-time coding based OFDM systems with QoS provision," in *Proc. IEEE Veh. Technol. Conf. (VTC'05),* Vol.4 pp. 2120-2123, Sept. 2005.

[25] C. Wei, L. Qiu and J. Zhu, "User Selection and Resource Allocation for Multi-User MIMO-OFDM Systems with Downlink Beamforming," in *Proc. IEEE Wireless Commun. and Networking Conf. in China (ChinaCOM'06),* pp. 1-5, Oct. 2006

[26] Y. H. Pan; S. Aissa, "Dynamic Resource Allocation for Broadband MIMO/OFDM Systems," in *Proc. IEEE Wireless Networks, Commun. and Mobile Computing Conf.,* Vol.2 pp. 863-867, Jun. 2005.

[27] A. Scaglione, P. Stoica, S. Barbarossa, G. B. Giannakis and H. Sampath, "Optimal Designs for Space-Time Linear Precoders and Decoders," *IEEE Trans. Sig. Proc.,* Vol.50, pp. 1051-1064, May. 2002.

[28] D. J. Love and R. W. Health Jr., "Limited Feedback Unitary Precoding for Spatial Multiplexing Systems," *IIEEE Trans. Sig. Proc.,* Vol.50 pp. 2967-2976, Aug. 2005.

[29] I. Emre Telatar, "Capacity of Multi-antenna Gaussian Channels," *AT&T Bell Laboratories, Internal Tech. Memo.,* June 1995.

[30] G. J. Foschini, "Layered space-time architecture for wireless communication in a fading environment when using multi-element antennas," *Bell Labs Tech. J.,* vol. 1, no. 2, pp. 41-59, Autumn, 1996.,

[31] S. M. Alamouti, "A Simple Transmit Diversity Technique for Wireless Communications," *IEEE J. Selec. Areas in Commun.,* vol. 16, no. 8, Oct. 1998.

[32] Q. H. Spencer, A. L. Swindlehurst and M. Haardt, "Zero-Forcing Methods for Downlink Spatial Multiplexing in Multiuser MIMO Channels," in *IIEEE Trans. Sig. Proc.,*,vol. 52, pp. 461-471, Feb. 2004.

[33] Z. Pan, K. K. Wong, and T.S. Ng, "Generalized Multiuser Orthogonal Space-Division Multiplexing," *IEEE Trans. Wireless Commun.,*vol. 3,pp. 1969-1973, Nov. 2004.

[34] C. Windpassinger, R. F. H. Fischer and J. B. Huber, " Lattice-reduction-aided broadcast precoding," *IEEE Trans. Commun.,*vol. 52,pp. 2057-2060, Dec. 2004.

[35] X. Qiu, K. Chawla, "On the Performance of Adaptive Modulation in Cellular Systems," *IEEE Trans. Commun.,* vol. 47, pp. 884-895, Jun. 1999.

[36] D. Kivanc and H. Liu, "Subcarrier allocation and power control for OFDMA," in *Conf. Rec. 34th Asilomar Conf. Signals, Systems and Computers,* vol. 1, pp. 147-151 , NoV. 2000.

[37] S. Pietrzyk, G. J. M. Janssen, A. N. Unit, P. T. C. Sp, and P. Warsaw, "Radio resource allocation for cellular networks based on OFDMA with QoS guarantees," in *Proc. IEEE Global Telecommunications Conf. (GLOBECOM'04),* vol. 4, pp. 2694-2699, Nov. 2004.

[38] J. Campello, "Optimal discrete bit loading for multicarrier modulation systems," in *Proc. IEEE Inform. Theory Symp.,* pp. 193, Aug. 1998.

[39] Y.J. Zhang and K.B. Letaief, "Optimizing Power and Resource Management for Multiuser MIMO/OFDM Systems," in *Proc. Global Telecommunications Conf. (GLOBECOM'03)*, vol. 1, pp. 179-183, Dec. 2003.

[40] J. Lee, R. V. Sonalkar and J. M. Cioffi, “Multi-user discrete bit-loading for DMT-based DSL systems,” in *Proc. IEEE Global Telecommunications Conf. (GLOBE-COM'02)*, Vol. 2, pp. 1259-1263, Nov. 2002.

[41] R. W. Heath Jr., S. Sandhu, and A. Paulraj, “Antenna selection for spatial multiplexing systems with linear receivers,” *IEEE Commun. Lett.,* vol. 5, no. 4, pp. 142-144, Apr. 2001.

[42] C. S. Park and K. B. Lee, “Transmit Power Allocation for BER Performance Improvement in Multicarrier Systems,” *IEEE Trans. Commun.* vol. 52, pp. 1658-1663, Oct. 2004.

[43] J.-Y. Liu and Y.T. Su, “Performance Analysis of Transform Domain Communication Systems in the Presence of Spectral Mismatches” , in *Proc. Military Commun. Conf. (MILCOM),* Orlando, FL., USA, Oct. 28-31, 2007.

[44] Y.-S. Lu, Y.-B. Lin, and Y.T. Su, “Dynamic Resource Allocation for Relay-Based OFDMA Systems with Fairness Considerations,” in *Proc. IEEE Wireless Commun. and Networking Conf. (WCNC)*, Sydney, NSW, Apr. 8-21, 2010.

[45] C.-L. Weng, Y.-B. Lin, and Y.T. Su, “Resource Allocation for MIMO-OFDMA Based Wireless Networks,” in *Proc. IEEE Wireless Commun. and Networking Conf. (WCNC)*, Sydney, NSW, Apr. 8-21, 2010.